Linking GCM-Simulated Climatic Changes to Ecosystem Models:

Case Studies of Statistical Downscaling in the Alps

Dimitrios Gyalistras, Hans von Storch,
Andreas Fischlin & Martin Beniston
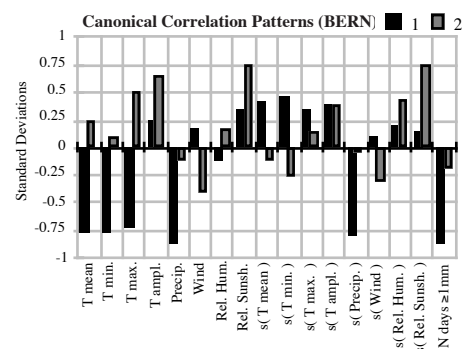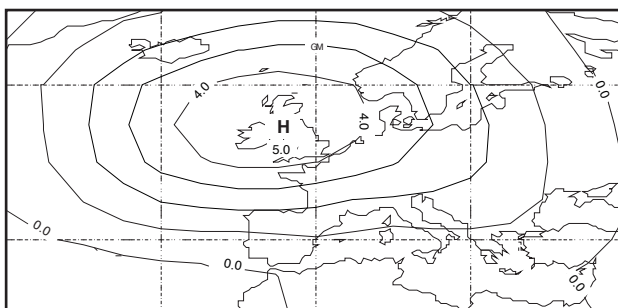
Juni/June 1994

Adressen der Autoren / Addresses of the authors:

D. Gyalistras & Dr. A. Fischlin
Systemökologie ETH Zürich
Institut für Terrestrische Ökologie
Grabenstrasse 3
CH-8952 Schlieren/Zürich
SWITZERLAND

e-mail: sysecol@ito.umnw.ethz.ch

Dr. H. von Storch
Max-Planck Institut für Meteorologie
Bundesstrasse 55
D-2000 Hamburg 13
F.R. GERMANY

e-mail: storch@dkrz.d400.de

Dr. M. Beniston
Institut für Geographie
ETH Zürich
Winterthurerstrasse 190
CH-8057 Zürich
SWITZERLAND

e-mail: beniston@ezrz1.vmsmail.ethz.ch

LINKING GCM-SIMULATED CLIMATIC CHANGES TO ECOSYSTEM MODELS: CASE STUDIES OF STATISTICAL DOWNSCALING IN THE ALPS

Dimitrios Gyalistras[1], Hans von Storch[2], Andreas Fischlin[3] & Martin Beniston[4]

Abstract

Based on the statistical approach proposed by VON STORCH *et al.* (1993), a general, flexible method to assess changes in the local climatic inputs of ecosystem models from large-scale climatic changes as simulated by General Circulation Models (GCMs) has been developed, verified and applied at five Swiss locations for the summer and winter seasons.

According to the requirements of various ecosystem models, at each location 17 seasonal statistics of daily temperatures, precipitation, sunshine duration, air humidity and wind-speed were considered. Year-to-year variations of the local variables were linked by means of Canonical Correlation Analysis to simultaneous anomalies of the North Atlantic/European sea-level pressure and near-surface temperature fields. The analysis was performed in the period 1901-40 and separately for each season and location. In all cases, physically plausible statistical models were found, which quantified the local effects of changes in major circulation patterns such as the strength of westerly flow in winter and of large-scale subsidence in summer.

In the verification interval 1941-80, most variables were better reconstructed in winter than in summer, and better at the three north alpine than at the two south alpine locations. The best reconstructed variables were seasonal mean daily temperatures and daily temperature extrema, for which at the different locations on average 42% – 75% of the total variances in the verification interval could be explained. Explained variances for precipitation totals were 29% – 55% in winter and 10% – 28% in summer, and for mean daily relative sunshine durations in both seasons ca. 12% – 53%. Seasonal mean relative humidities, mean wind speeds, and within-summer standard deviations of daily variables were generally poorly reproduced. It was found that the procedure of VON STORCH *et al.* (1993) can be generally improved by using in addition to sea-level pressure the near-surface temperature as a large-scale predictor. Improvement was strongest for temperature related variables, and for the summer season.

The established statistical relationships were applied to anomaly fields as simulated by the ECHAM1/LSG-GCM under increasing atmospheric greenhouse-gas concentrations. The procedure yields for several important ecosystem inputs time-dependent, internally consistent, and regionally strongly differentiated climatic change estimates at a spatial resolution far above the resolution of present GCMs.

[1, 3] Systems Ecology, Swiss Federal Institute of Technology Zurich (ETHZ), Institute of Terrestrial Ecology, Grabenstrasse 3, CH-8952 Schlieren, Switzerland.

[2] Max-Planck Institut für Meteorologie, Bundesstrasse 55, D-2000 Hamburg 13, F.R. Germany.

[4] Institute of Geography, Swiss Federal Institute of Technology Zurich (ETHZ), Winterthurerstrasse 190, CH-8057 Zurich, Switzerland.

1. INTRODUCTION

In order to study possible impacts of climatic change on particular ecosystems, models of these systems are of paramount importance. Although ecosystems and the atmosphere interact on a multitude of temporal and spatial scales, most impact studies consider only the "one-way" forcing of the ecosystems by the atmosphere, yet in an impressive variety.

Typically ecosystem models require input data on meteorological variables such as temperature, precipitation, photosynthetically active radiation, wind, and air humidity. For example, agro-ecosystems (PARRY et al., 1988; SPITTERS et al., 1989; ROTH et al., in print) or insect population models (LISCHKE & BLAGO, 1990) need several meteorological variables with an hourly to daily time step for at least the duration of the vegetation season. On the other hand, forest gap models (SHUGART, 1984) simulating forest succession require realisations of monthly mean temperatures and precipitation totals for every month of the year (FISCHLIN et al., in print), or the population dynamics model for red deer by SCHRöDER (1976) requires monthly snow-heights.

To study and assess the impacts of climatic change, a given set of such inputs needs to be derived from appropriate climatic change scenarios. A scenario at a particular location and moment should represent an internally consistent picture for changes in at least those climatic parameters which are needed either as direct model inputs (FISCHLIN, 1982; BRZEZIECKI et al., 1993), or to stochastically generate the weather variables that drive the ecosystem model (e.g. MEARNS et al., 1984; SUPIT, 1986; SWARTZMAN & KALUZNY, 1987; WILKS, 1992; FISCHLIN et al., in print).

Appropriate climatic change scenarios should extend from presence far enough into the future, or otherwise cover long enough time spans. In some cases, e.g. agroecosystems, a few decades can be sufficient. When however soils or forests are considered, which have time constants of several centuries (BUGMANN & FISCHLIN, 1992; 1994), the scenarios should specify the transient behavior of regional climates for at least a few hundred years.

Further, the climatic inputs are typically needed at specific representative locations, i.e. with a spatial resolution of a few kilometres or less. A high spatial resolution is of particular importance if ecosystems are studied within a complex topography such as the Alps.

Three basic approaches could be adopted to derive the needed regional climatic change scenarios (GIORGI & MEARNS, 1991): a) Construct regional climatic change analogues from past climatic situations as inferred from proxy data (FLOHN & FANTECHI, 1984; WIGLEY et. al, 1986) or instrumental records (e.g. WIGLEY et. al, 1980; PITTOCK & SALINGER, 1982; LOUGH et. al; 1984; HULME et. al; 1990). b) Use numerical models, such as General Circulation Models (GCMs) or limited area meteorological models (LAMs; e.g. GIORGI et al., 1990) embedded in GCMs, to simulate possible future climatic conditions with the best possible spatial detail. c) Use, as an in-between solution, semiempirical approaches establishing a statistical relationship between larger-scale and regional climatic changes (e.g. KIM et al., 1984; WILKS, 1989) which then can be applied to derive climatic change scenarios from the outputs of spatially coarse numerical models (WIGLEY et al., 1990; KARL et al., 1990; VON STORCH et al., 1993).

A major advantage of the first, purely empirical, approach is that it is relatively simple to implement. However, paleoclimatic analogues normally provide information only on few parameters, such as mean temperatures and, less often, precipitation (WIGLEY et. al, 1986). In addition, the temporal resolution of proxy data is often coarse, and, even if yearly data are available (e.g. from tree rings), the annual cycle may not be well resolved (STOCKTON et al., 1985; SCHWEIN-GRUBER, 1988). Though this is not the case for instrumental records, there still remains the problem that past climatic changes do not necessarily reflect the effects of increasing greenhouse gas concentrations on climate (GIORGI & MEARNS, 1991). Also, due to the lack of deterministic models it is difficult to formulate gradual shifts in future climates in a physically consistent manner.

The second approach relies upon GCMs. Since GCMs reproduce most large-scale atmospheric and oceanic features, present – and even more so future – climate models are regarded as being capable to reliably simulate at least the broad large-scale aspects of man-made climatic change (DICKINSON, 1986; GATES *et al.*, 1990). Simulations of time-dependent changes for the next 100 years or so become increasingly available (MANABE *et al.*, 1991, 1992; CUBASCH *et al.*, 1992; GATES *et al.*, 1992), hereby providing vast amounts of physically consistent data with a time step of one hour or less.
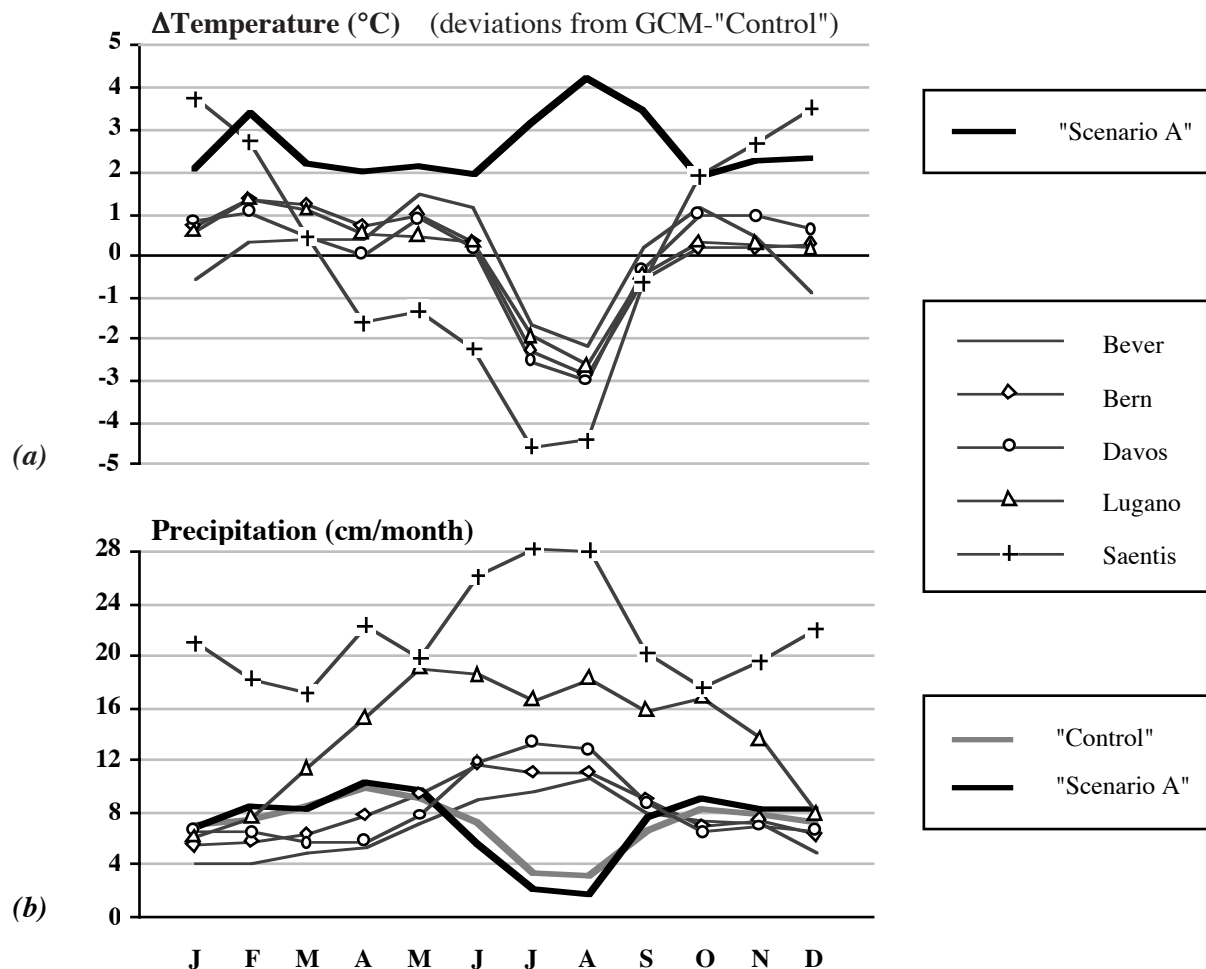
Fig. 1: Comparison between the climate simulated by the ECHAM1/LSG-GCM in the vicinity of the Alps (averages from three gridpoints) and observations. (a) Monthly mean temperatures. Thick line: differences between the means simulated in the years 2075-2084 of the GCM-"IPCC Scenario A" experiment and the means from the "control" experiment. Thin lines: deviations of observations from the "control". The following annual mean temperatures were subtracted prior to the calculation of the deviations: Bever: 1.5°C, Bern: 8.4°C, Davos: 3.0°C, Lugano: 11.7°C, Saentis: -2.1°C, "control": 8.7°C. (b) Monthly precipitation totals. Thick lines: simulated annual cycles. Thin lines: observed annual cycles.

However, a problem occurs due to the coarse horizontal resolution of most currently used climate models, which is in the order of 500 km, and which sharply contrasts with the fine resolution required by ecosystem models. Furthermore, the minimum spatial scale at which GCMs produce skillful results lies above several gridpoint distances. For present GCMs this is at least 2'000 - 4'000 km (VON STORCH *et al.*, 1993). Climatic changes obtained at individual gridpoints seem even less trustworthy over mountainous areas such as the Alps, which are not well represented in GCMs. This is illustrated in Fig. 1 which compares the performance of the ECHAM1/LSG-GCM at three gridpoints in the vicinity of the Alps with measurements from the

five case study locations considered in this study. Though in the GCM-"control" experiment (simulation of present climate) the observed annual cycle of temperature is reproduced qualitatively correct, with a flat maximum in July/August and a minimum in January (not shown), the GCM generally overestimates the amplitude of the annual cycle by several degrees. In particular note, that the differences between the observations and the gridpoint-simulated values are of similar size as the temperature changes simulated at the gridpoints for the years 2075-2084 under increased greenhouse gas concentrations (Fig. 1a). Precipitation is at all locations severely underestimated during the summer months. Again, the projected changes in gridpoint precipitation are much smaller than the deviations typically found between the observations and the "control" (Fig. 1b).

One possibility to improve the simulation of regional climates is to increase the horizontal resolution of the GCMs or, at least, to use them to drive simulation models with enhanced resolution over areas of interest (LAMs). Computational costs of climate models increase however at least quadratically with the spatial resolution (GIORGI & MEARNS, 1991). It may therefore be expected that, even if more powerful computers become available, the simulation of the full annual cycle over several decades, let alone centuries, by high-resolution models will not be possible for several years to come. Furthermore, even if gridpoint distances for long-term integrations could be reduced to 100 km or less, there would still remain a substantial gap between the skillful scales of the climate models and the local detail required by most ecosystem models.

An alternative is to use semiempirical approaches which allow to combine site-specific empirical data with the physically consistent results of numerical climate models. Semiempirical approaches are particularly attractive, since, in principle, they can be flexibly used at any location and for any variable of interest. Moreover, thanks to their computational efficiency they would even allow to derive transient scenarios far into the future.

Several semiemprical approaches have been proposed till now. For example, WIGLEY et al. (1990) used monthly means of several regionally averaged atmospheric variables to predict monthly mean surface temperature and precipitation perturbations at the 32 climate stations within the region considered; KARL et al. (1990) related daily gridpoint data of 22 free-atmosphere variables to daily temperature extrema, precipitation and cloud ceilings from local surface observations; VON STORCH et al. (1993) used anomalies of large-scale mean sea-level pressure over the Atlantic to predict by means of Canonical Correlation Analysis (BARNETT & PREISENDORFER, 1987) changes in winter mean Iberian precipitation; finally, WERNER & VON STORCH (1993) used basically the same approach to relate January-February mean temperatures from 11 Central European stations to the large-scale circulation.

The method of VON STORCH et al. (1993) appears to be superior, because, unlike the other approaches, it considers the large-scale (several 10^3 km) behavior of a climatic parameter, according to the assumption that predictions of future climates by GCMs are most credible within this resolution. Also, unlike the approach by KARL et al. (1990), the statistical models obtained do not depend on a particular GCM and can thus be flexibly applied to several GCMs. However, the method of VON STORCH et al. (1993) has so far been applied only to predict one climate variable at a time, i.e. rainfall or temperature, and only for winter.

Thus the following questions arise: Is it possible to establish plausible statistical relationships which allow to link multivariate descriptions of local climates, and even in a complex orography like the Alps, to large-scale climatic changes? If yes, for which ecosystem inputs, seasons and locations can be obtained the best and for which the poorest results? What improvements could be gained by modifying the method, for instance by including large-scale near-surface temperature anomalies as an additional predictor? Finally, is it possible to derive from GCM projected global climatic changes regionally differentiated scenarios?

In this paper the method by VON STORCH et al. (1993) was used for the first time to downscale with a seasonal resolution, not only for winter, but also for summer, large-scale climatic changes to 17 local ecosystem inputs at several point locations within a complex topography, i.e. at five

representative case study locations in the Alps. We show that the method proposed by VON STORCH *et al.* (1993) not only yields physically plausible results for all case study locations, but that it can also be substantially improved, in particular for temperature-related variables. Finally, by applying the obtained statistical relationships to two climatic change experiments with a GCM, we demonstrate that our approach allows to derive regionally differentiated, transient climatic change scenarios of use to ecosystem studies.

2. DATA AND METHODS

2.1 Observations

As independent variables (predictors) have been tested mean sea-level pressure (SLP) and two-meter above ground air temperature for which long-term (several decades) observed data sets are available. The independent variables were given on a 5° x 5° latitude by longitude grid containing 153 gridpoints and extending from 40°W to 40°E and 30°N to 70°N (Fig. 2a).

Winter (DJF) and summer (JJA) mean SLP for the years 1901-80 were calculated at each gridpoint from daily data provided in the NCAR data set (JESSEL, 1991). Seasonal mean near-surface (two meter above-ground) temperatures were derived for the same period from monthly data given on a 10° x 5° latitude by longitude grid (VINNIKOV, 1986; JESSEL, 1991), and were then interpolated to the 5° x 5° standard grid. Missing data for some years and gridpoints were replaced by interpolation between adjacent timepoints.
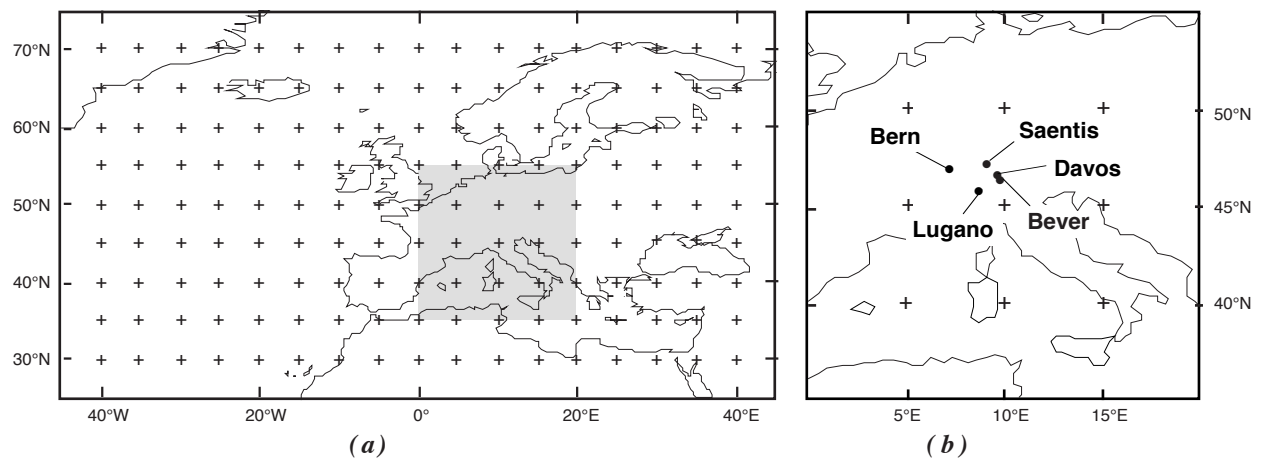
Fig. 2: (a) Gridpoints of sea-level pressure and near-surface temperature fields used in this study. (b) The five Swiss locations considered.

The SLP data were initially given as absolute values, whereas the near-surface temperature data were given as anomalies from the three different basis periods 1881-1935, 1881-1940 and 1881-1960. However, since fitting of the statistical models required data with zero means, anomalies were calculated for both predictors relative to the mean states of the respective years used (see also statistical method, below).

On the regional scale, five different locations within Switzerland, representative of north, inner and south alpine climates were considered (Fig. 2b): (1) Bern (valley, 565 m.a.s.l., 7.4° E 46.9° N) at the northern slope of the Alps; (2) Davos (pronounced valley location, 1590 m.a.s.l., 9.8° E 46.8° N) in the central alpine region; (3) Bever (1712 m.a.s.l., 9.9° E 46.6° N), located in the Oberengadine valley which can be attributed to central or south alpine climate; (4) Lugano (valley, 273 m.a.s.l., 9° E 46° N) at the southern slope of the Alps; and (5) Saentis (mountain

peak, 2500 m.a.s.l., 9.4° E 47.3° N) which represents "free-atmosphere" conditions at the northern side of the Alps.

Meteo Variable	Seasonal Statistics	Explanations
Temperature	(a) Tmean, Tmin, Tmax, Tampl (b) s(Tmean), s(Tmin), s(Tmax), s(Tampl)	(a): means, (b): standard deviations of daily mean, minimum and maximum temperatures and of daily temperature amplitude, respectively (in °C).
Precipitation	(a) Precip (b) s(Precip) (c) Ndays≥1mm	(a): mean, (b): standard deviation of daily precipitation totals (in cm); (c): number of days with total greater than one mm.
Relative sunshine duration	(a) Rel.Sunsh. (b) s(Rel.Sunsh.)	(a): means, (b): standard deviations of respective daily averages from three measurements per day (in %).
Relative humidity	(a) Rel.Hum. (b) s(Rel.Hum.)	(in %)
Wind speed	(a) Wind (b) s(Wind)	(in m/sec)

Table 1: Meteorological variables and their seasonal statistics considered.

The dependent variables (predictands) were given at each location by a vector of 17 seasonal weather statistics (Table 1). Special notice was given to the main weather elements temperature and precipitation which were credited together 11 variables. Relative sunshine duration was included as a variable allowing to approximate incoming photosynthetically active radiation which determines in many ecosystem models rates of plant growth. As additional parameters needed in particular by agroecosystem models we considered relative air humidity and wind speed. Within-season standard deviations of all meteorological variables were included as parameters typically needed to simulate daily weather conditions by means of stochastic weather generators. Since precipitation distributions often show considerable skewness, we used as an additional parameter for the within-season variability of rainfall the number of days with precipitation ≥ 1mm, which is proportional to the probability of "wet days" within the season. The threshold value of 1mm was chosen because it represents a lower limit for the detection of rainfall valid for most measuring devices (cf. UTTINGER, 1965).

All seasonal statistics were derived from daily 1901-80 measurements, extracted from the database of the Swiss Meteorological Institute (SMA), Zurich (SMA, 1901-80; BANTLE, 1989). Daily mean temperatures, relative sunshine durations, relative humidities and wind speeds, were calculated from three measurements per day, whereas daily temperature minima and maxima were determined as the extrema from the three daily measurements and the evening temperature of the previous day. After 1971 the timepoint of the evening temperature measurements has been changed from 21:30 to ca. 19:00, for which reason daily means for the years 1901-1970 and 1971-80 were calculated according to different procedures (BANTLE, 1989). The effects of this change in procedures are still under investigation by the SMA; for locations with large daily temperature amplitudes it is likely that due to the new procedure daily mean temperatures are overestimated by ca. 0.2° C (A. DE MONTMOLLIN, SMA, pers. comm.).

2.2 GCM-Experiments

Simulated seasonal mean SLP and near-surface temperature were obtained from experiments performed with a fully coupled global atmospheric/oceanic GCM run at the Max-Planck Institute for Meteorology (MPI), Hamburg. The atmosphere component (ECHAM1) of the model is a version of the spectral numerical forecasting model of the European Centre for Medium Range Weather Forecasts extensively modified at the MPI Hamburg for climate simulations. Its horizontal resolution is limited by a cut-off at wave number 21, corresponding to a gaussian grid

with an average spacing of 5.6°, and its vertical resolution is given by 19 levels in a hybrid σ-p-system. The ECHAM1 model simulates the diurnal cycle with a time step of 40 minutes. The ocean component (LSG), which allows for the calculation of large scale geostrophic motions, is based on 11 variably spaced vertical levels, an effective horizontal grid-size of 4° and a basic time step of 30 days (for the two uppermost ocean layers and interaction with the atmosphere: 1 day). A more detailed description of the coupled model is given in CUBASCH et al. (1992).

All GCM-simulated data used in this study were derived from daily GCM-outputs and were interpolated on the 5° x 5° grid of the observed data sets. We considered results from (1) the "control" integration with constant 1985 atmospheric CO_2-concentration, (2) the "double CO_2" (DCO2) experiment representing the model system's response to a step doubling of greenhouse gas concentrations from 360 to 720 ppm equivalent CO_2, and (3) the "IPCC Scenario A" (SCNA) experiment, where the GCM is forced by time-dependent greenhouse gas emissions according to the "Business-As-Usual" scenario given by HOUGHTON et al. (1990). The model's performance in the "control" run and its responses to the greenhouse gas forcings are addressed later.

2.3 Statistical Procedure

Our method is based upon a "Perfect Prog" approach (GLAHN, 1985; VON STORCH et al., 1993). A statistical relationship is first established between the large-scale and the local observations, and then applied unmodified to predict changes in the local variables from any large-scale observations, or GCM-simulated data sets. Hereby, each season and location was considered separately.

The overall procedure consists of (1) the selection of two subperiods used to fit respectively verify the statistical models, (2) the calculation of anomalies, plus the weighting of the predictor and predictand variables, (3) the estimation of a series of differently specified statistical models linking the two data sets to each other, (4) the verification of all specified models with independent observations, (5) the selection of a subset of the best-performing models, and finally (6) the application of the selected models to GCM anomaly-fields (Fig. 3).

In the standard procedure we used the years 1901-40 for model estimation and the years 1941-80 for model verification. In order to test the sensitivity of the resulting climatic change scenarios to the choice of the estimation period, the two subperiods were reversed at a later stage.

All variables were transformed to deviations from the mean states of the years used for model estimation. This is because only anomalies of the large-scale and local variables were related to each other, whereas the long-term means were not affected by the procedure. On the local side, this ensures that climatic change scenarios can be specified consistent with present long-term mean climate at each location, whereas on the side of the large-scale predictors only the changes occurring between a climatic change experiment and the "control" experiment of a GCM need to be considered. The use of anomaly fields avoids the problem that the long-term mean fields simulated by GCMs are normally biased with respect to observations.

The predictor variables were weighted with the square root of their latitude cosine, in order to account for the latitudinal variation of the grid-box sizes of the rectangular 5° x 5° grid. When both, SLP and near-surface temperature, were used as predictors, each field was rescaled with a constant factor in order to account for a prescribed proportion (e.g. half) of the total predictor variance. For graphical representations of predictor patterns however, all weightings were removed, such that the same unit applied to all variables of the same kind. The local weather statistics were weighted with their observed standard deviations from the years used for model estimation, thus eliminating the effects of different value ranges.
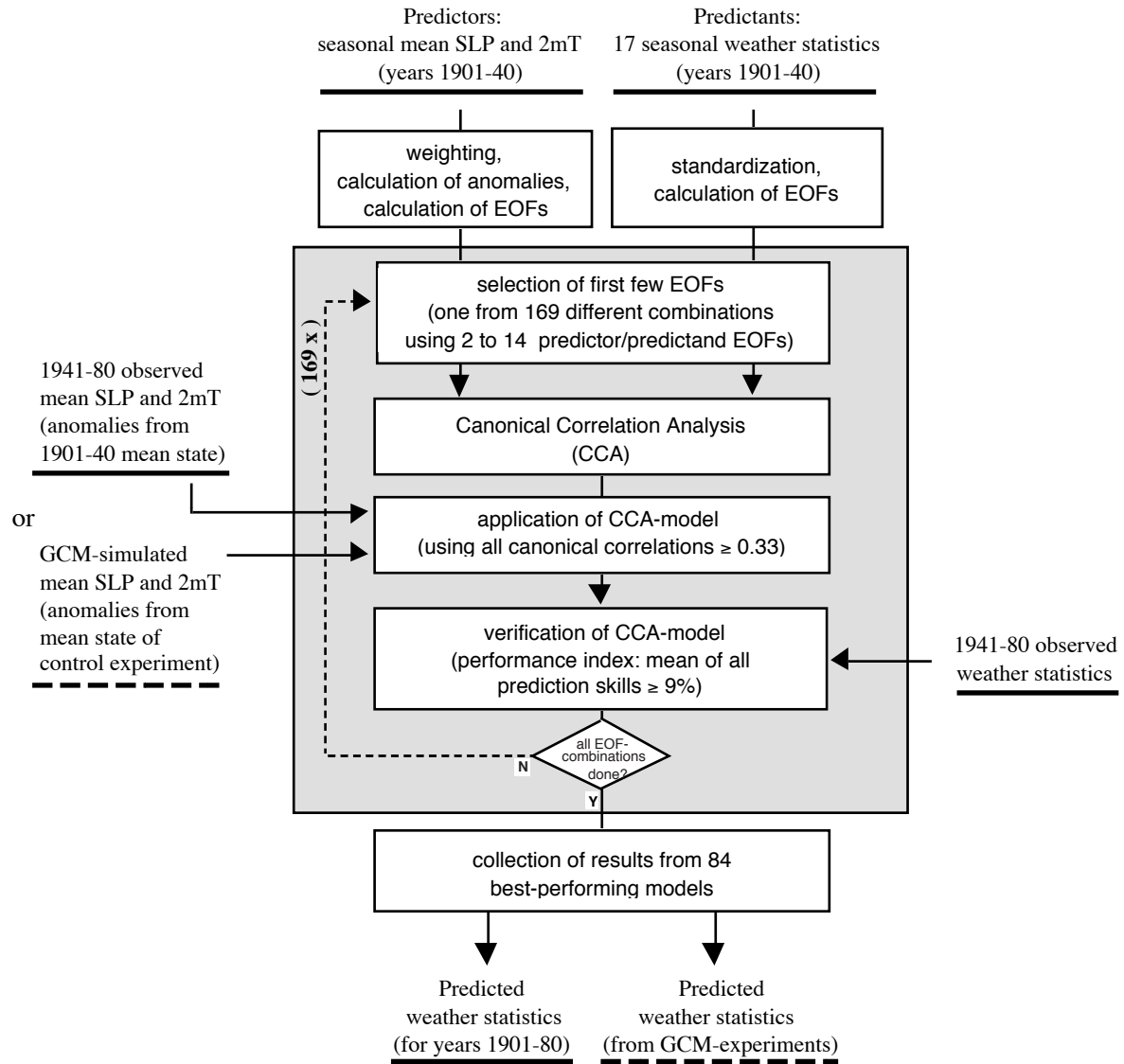
Fig. 3: Block diagram of the method used to derive local climatic change scenarios from large-scale climatic changes as simulated by GCMs. Underlined texts = input/output data sets; boxes = procedures; solid lines with arrows = flow of data; dashed line with arrow = iteration over procedures within grey box. For more explanations see text.

Estimation of the statistical models consisted of two parts: first, dimensionality of the observed data sets was reduced and linear dependencies between variables within the same data set were removed by estimating separately for the n_x predictors x_j ($j=1..n_x$) and for the n_y predictands y_k ($k=1..n_y$) the eigenvectors of the respective 2nd-moment matrices, i.e. the empirical orthogonal functions (EOFs; e.g. KUTZBACH, 1967; EHRENDORFER, 1987). Then, the time coefficients (i.e. the estimated principal components or PCs) of the first e_x predictor and the first e_y predictand EOFs were related by means of Canonical Correlation Analysis to each other (CCA; e.g. ANDERSON, 1984; BARNETT & PREISENDORFER, 1987). Based on the eigenvectors of the squared covariance matrix of the PCs, CCA identifies $n_c = Min(e_x, e_y)$ linear combinations of the predictor PCs which correlate best with respective linear combinations of the predictand PCs. The scalars determining these linear combinations were transformed from the EOF- back to the physical space, yielding n_c *canonical patterns* P_i and Q_i ($i=1..n_c$) for the predictors and predictands, respectively. Each pair of patterns corresponds to a *canonical mode*. The canonical patterns were used to infer from the x_j and y_k two new sets of variables, the *canonical time coefficients* s_i and t_i ($i=1..n_c$) according to the equations

$$s_{i(t)} = \sum_{j=1}^{n_x} P'_{ij} \cdot x_{j(t)} \quad (1) \qquad \text{and} \qquad t_{i(t)} = \sum_{k=1}^{n_y} Q'_{ik} \cdot y_{k(t)} \quad (2),$$

respectively. (Primes denote transposition of a matrix). The P_i and Q_i are determined by CCA under the constraint that all s_i as well as all t_i are mutually uncorrelated, but that the first pair of time coefficients (s_1,t_1) shows a maximum *canonical correlation* ρ_1. Every further pair (s_m,t_m) of time coefficients, correlating with a factor ρ_m (m=2..n$_c$), can be used to explain a maximum of the remaining variance of the respective data sets.

When using both, SLP and near-surface temperature, as predictors, the x_j may be subdivided into SLP-anomalies (j=1..153) and near-surface temperature-anomalies (j=154..306). Accordingly, an individual pattern P_i was visualised as composed of two separate maps defined by the corresponding elements P_{ij}. The associated time coefficient s_i may be given as the sum of two signals:

$$s_{i(t)} = \sum_{j=1}^{153} P'_{ij} \cdot x_{j(t)} + \sum_{j=154}^{306} P'_{ij} \cdot x_{j(t)} \qquad\qquad (1')$$

Due to the respective orthogonality of the s_i and t_i, the element P_{ij} (or Q_{ik}) of the i-th canonical pattern represents the covariance between the j-th predictor (the k-th predictand) and the dimensionless coefficient s_i (t_i). Local maxima (minima) in the predictor maps of the i-th canonical mode represent thus regions where positive (negative) anomalies in the respective x_j contribute with large positive anomalies to the coefficient s_i (cf. Eq. 1 or 1'). Similarly, a large positive (negative) value Q_{ik} denotes that for the i-th canonical mode a large positive (negative) anomaly of the k-th weather statistic occurs, if the time coefficient t_i takes a positive value. Finally, the canonical correlation ρ_i between s_i and t_i measures the strength with which anomalies in the predictands and predictors are related to each other within the respective canonical mode.

The results of CCA can be used to linearly predict from any anomaly fields describing changes in the predictors x_j the simultaneous responses of all local weather statistics y_k (k=1..n$_y$), according to

$$y^*_{k(t)} = \sum_{i=1}^{n_{cu}} t^*_{i(t)} \cdot Q_{ik} = \sum_{i=1}^{n_{cu}} \rho_i \cdot \frac{\sigma_{s_i}}{\sigma_{t_i}} \cdot s_{i(t)} \cdot Q_{ik} \qquad (3)$$

Here, $n_{cu} \le n_c$ is the number of canonical modes used, t_i^* denotes the estimated i-th time coefficient of the dependent variables, and σ_{s_i}, σ_{t_i} are the standard deviations of the time coefficients $s_{i(t)}$ and $t_{i(t)}$, respectively. For each CCA model fitted, we chose n_{cu} individually as the number of all canonical correlations ρ_i above the threshold value $\eta_c = 0.33$. For the choice of η_c we assumed that serial correlation in the predictors and predictands can be neglected due to the interannual variations considered. Given that CCA systematically overestimates the true ρ_i, η_c was hereby chosen larger than the critical value of 0.26 (0.31) above which an unbiased estimate of a correlation coefficient would be significantly different from zero at the 90% (95%) confidence level (two-sided t-test, n=40; e.g. KREYSZIG, 1977).

Performance of CCA may sensitively depend on the numbers e_x and e_y of EOFs considered. Using a too large number of EOFs will fit the statistical models too strongly to the particular data sets considered, most probably missing an adequate description of the underlying stochastic process. A too small number of EOFs on the other hand will omit part of the significant signal, thus resulting in a poorer predictive ability of the overall model. As an alternative to the identification of a significant, fixed number of EOFs to be retained by means of EOF-selection rules (e.g. PREISENDORFER *et al.*, 1981) in this study we rather focused on the effects resulting from possible alternative choices for e_x and e_y. To this purpose we performed CCA for the 13^2=169

combinations resulting when varying e_x and e_y individually within the range of 2..14. The upper limit of 14 EOFs was chosen because from this number on typically more than 90% of the total variances of the predictor and predictand data sets could be accounted for, for all seasons and locations considered.

Each of the 169 CCA models was applied to predict the local variables from the large-scale data not used for model estimation, and model performance was assessed according to

$$\Psi_{(e_x,\ e_y)} = \frac{1}{n_y} \cdot \sum_{k=1}^{n_y} \text{Max} \left(0,\ \text{Cor} \left(y_{k(t)},\ y^*_{k(t)} \right) - \eta_v \right) \qquad (4)$$

Ψ measures the mean of all correlations above the threshold value $\eta_v = 0.3$ between the observed (y_k) and reconstructed (y^*_k) weather statistics in the 40-year verification period. The value chosen for η_v can be justified similarly as was done for η_c above.

The 84 (= half of 169) best-performing models were then used to evaluate the performance of the procedure for the individual weather statistics, and to derive climatic change scenarios from the GCM-experiments.

3. RESULTS AND DISCUSSION

3.1 Model Estimation

We investigated five different variants of predictor data sets, with the SLP and near-surface temperature fields accounting for the total variance of all predictors as given by the ratios 1:0 (i.e., only SLP), 2:1, 1:1, 1:2 and 0:1 (only temperature). For the predictors being SLP alone, SLP and near-surface temperature with equal weight, and temperature alone, respectively, the canonical patterns and time coefficients of individual CCA models were graphically represented and visually compared under each other and between locations.

In this subsection we mainly present results for the example location of Bern, since results obtained for Bever, Davos, Lugano and Saentis could be interpreted similarly as this is done for Bern below. We also present only CCA models fitted to a combined predictor data set (SLP and near-surface temperature with equal weight), because the canonical patterns resulting when using only one field were found quite similar to the respective subpatterns of the combined approach. This was generally the case for both seasons considered.

a) Winter

Fig. 4 shows the CCA model obtained for $e_x = e_y = 4$ for Bern in winter. The first predictor pattern consists of a large positive SLP anomaly centred over Britain, a negative temperature anomaly over lands, and a positive temperature anomaly over the Atlantic with an increasing amplitude towards north-west. The two subpatterns give a consistent picture: in winters with on average higher than normal pressure over Britain, mean westerly flow and thus advection of relatively mild maritime air towards the continent are less pronounced, such that temperatures over lands drop below their long-term means. At the same time, advection of polar air into the north-west Atlantic is also reduced, resulting in above-normal temperatures in this region. This was the dominant predictor pattern in winter for all locations considered.

The first canonical pattern of the weather statistics in Bern (Fig. 4c, black bars) confirms the above interpretation: temperatures are anomalously low, as are precipitation, its standard deviation, and the number of days where precipitation exceeds 1mm. The negative responses in the precipitation-related variables are plausible, indicating that advection of maritime air is the main

source of winter precipitation in Bern. Since the sign of the canonical patterns is arbitrarily determined by CCA, note that the following interpretation also holds: a negative SLP-anomaly centred over Britain, indicating intensified mean westerly flow, goes with anomalously high temperatures over the continent, and also implies positive temperature and precipitation anomalies in Bern.
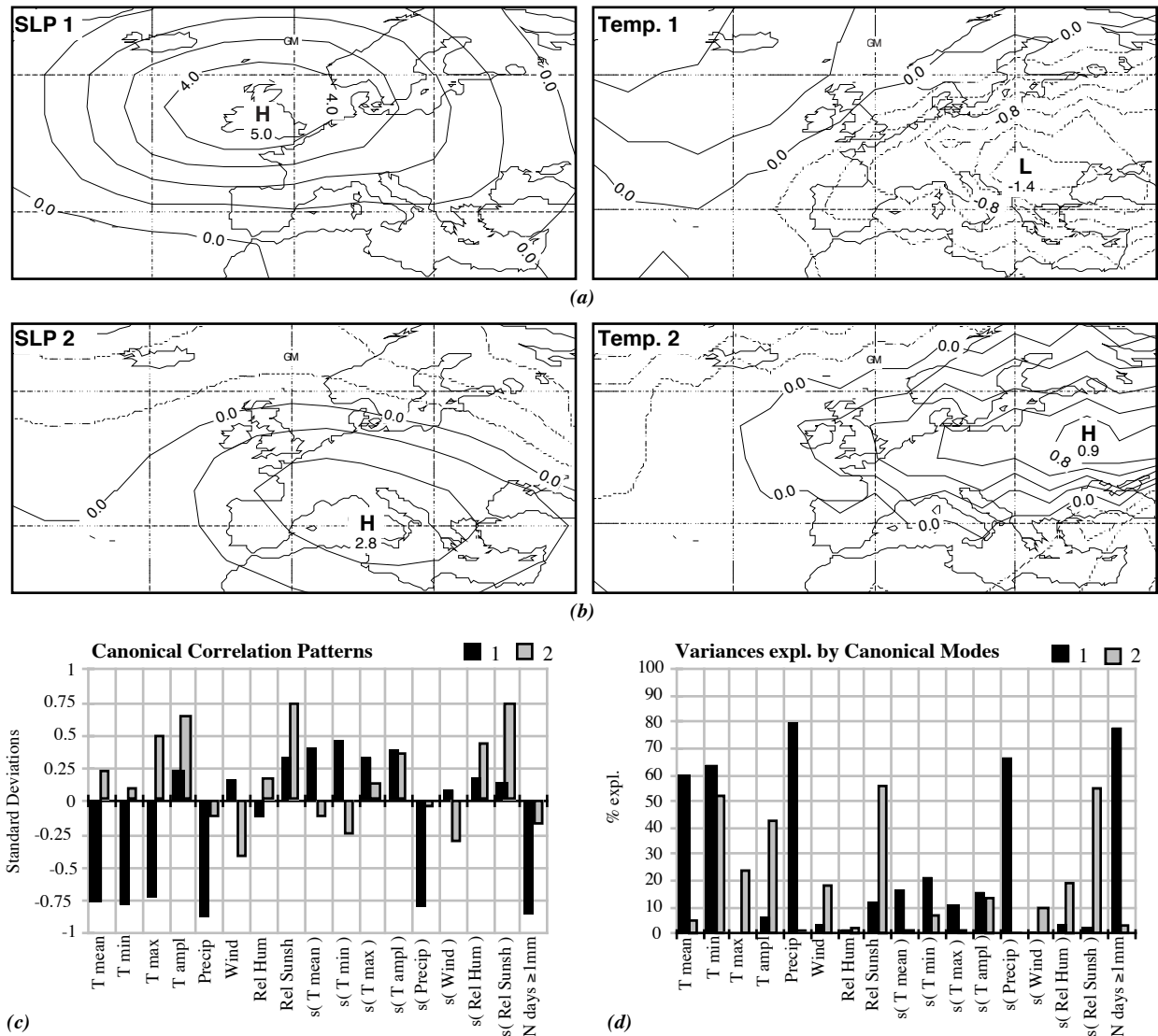

Fig. 4: CCA model for Bern in winter. (a) first, (b) second canonical pattern for the predictors. *Left* sides of (a) and (b): SLP subpatterns, contour-interval 1 mb. *Right* sides: near-surface temperature subpatterns, contour-interval: 0.2°C. (c) canonical patterns, (d) explained variances for the local weather statistics. The first 4 predictor EOFs and the first 4 weather statistics EOFs were used, explaining approx. 75% and 77% of the respective total variances. Correlations between time coefficients are 0.89 for the first and 0.82 for the second mode.

The relevance of the large-scale patterns for the individual weather statistics can be seen from Fig. 4d. Shown are the proportions of the variances of the local variables which were explained by the time coefficients $t_{1(t)}$ (black bars) and $t_{2(t)}$ (grey bars), i.e. the squared correlation coefficients (in percent) between the $y_{k(t)}$ and $t_{i(t)}$ for the model estimation period 1901-1940.

The second canonical mode mainly explained the variability of winter mean daily temperature amplitudes, mean relative sunshine duration, and its within-season standard deviation (Fig. 4d,

grey bars). Positive anomalies in those variables (Fig. 4c, grey bars) correlate with anomalously high SLP over Southern Europe (Fig. 4b, left), implying intensified mean advection of warm air from west/south-west, and thus elevated temperatures over the continent with a maximum over Eastern Europe (Fig. 4b, right). The responses of the weather statistics are consistent, since predominance of high pressure over Central/Southern Europe means also for Bern more frequent occurrence of cloudless winter days, with more sunshine, but also with larger radiative energy loss during the nights, resulting in higher daily temperature amplitudes.

(a)

(b)

(c)   *(d)*
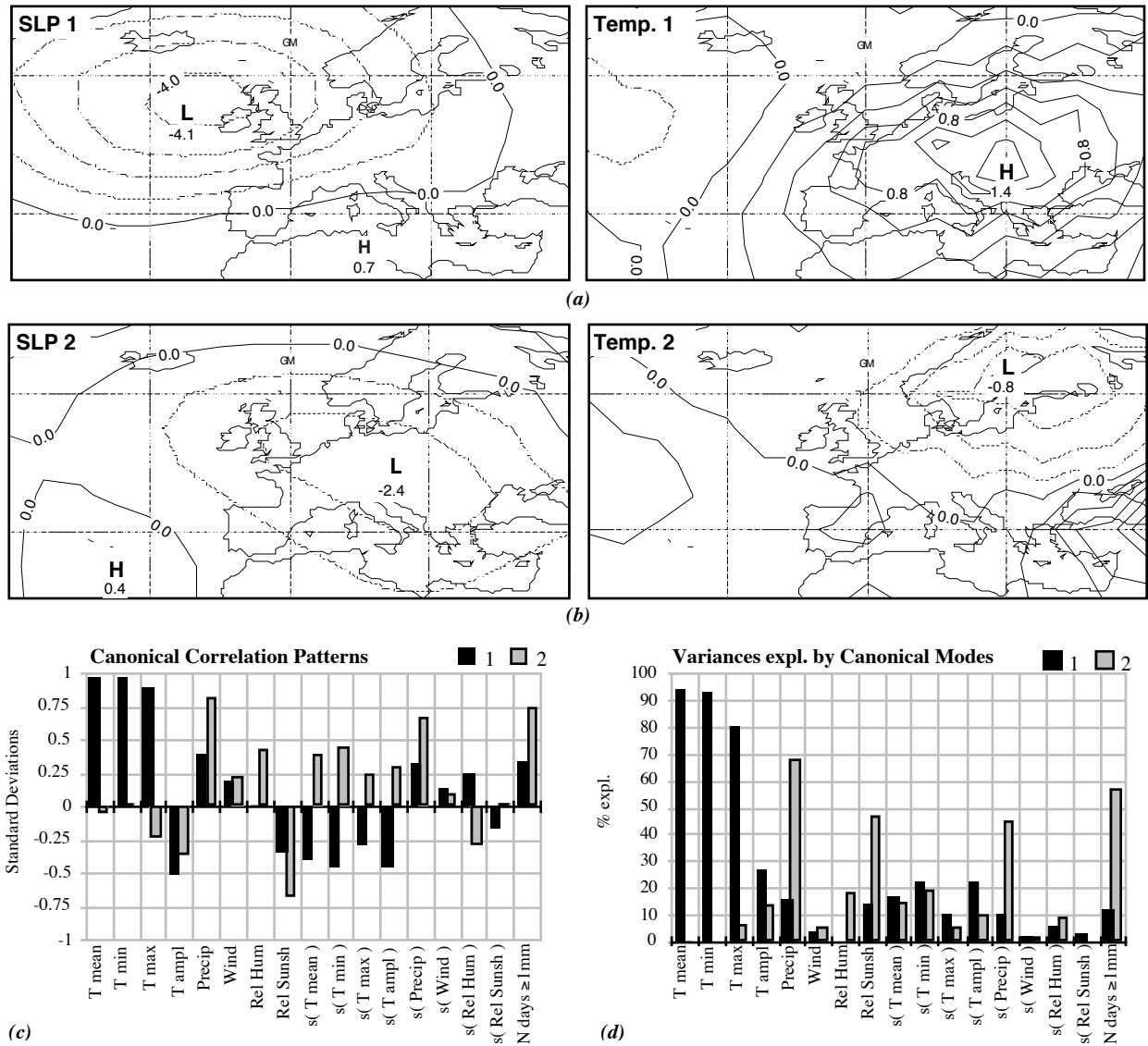
Fig. 5: Same as Fig. 4, but for Davos. The first 7 predictor EOFs and the first 4 weather statistics EOFs were used, explaining approx. 88% and 73% of the respective total variances. Correlations between time coefficients are for the first mode 0.91, for the second 0.79.

The third and fourth canonical modes (not shown) also contributed to the explanation of the year-to-year variability of the weather statistics. The third predictand pattern denoted predominance of meridional flow from north/north-east, which at Bern was associated with below-normal temperatures and mean wind speed, with higher than normal within-season temperature variability, and increased relative humidity. The fourth predictand pattern showed a large positive SLP anomaly over mid-latitude Atlantic and corresponding large-scale positive near-surface temperature anomalies over Finland; it mainly correlated with negative deviations in the within-

season standard deviations of daily temperature means and extremes. The third and the fourth mode showed canonical correlations of 0.55 and 0.37, respectively,, such that they also contributed to the reconstruction of the weather statistics in the model verification phase.

The canonical correlation patterns obtained for Davos (Fig. 5) illustrate the regionally differentiated relationships established by means of CCA. In contrast to Bern, year-to-year variations of winter mean precipitation, its within-season standard deviation, and of the probability of precipitation events ≥ 1mm (Fig. 5d, grey bars) were in Davos mainly explained by the second canonical mode (cf. Fig. 5b), not by the mean strength of westerly flow. In addition, though the respective SLP and temperature subpatterns are qualitatively similar for Bern and Davos, regional differentiation may also be given by shifts in the locations and/or amplitudes of the pattern's troughs and ridges. Due to sampling uncertainties however, it could be that not all respective patterns are significantly different from each other.

b) Summer

Fig. 6 shows the results of CCA with $e_x = 4$ and $e_y = 3$ for Bern in summer. Again, the first predictor pattern depicted here for Bern was typical for all other locations as well. Its SLP-sub-pattern (Fig. 5a, left) shows over Europe a quantitatively small positive anomaly (ca. 0.7 mb) when compared to the 1901-80 standard deviation of mean summer SLP, which ranges from approximately 0.8 mb over the Mediterranean area to ca. 2 mb over Britain and Scandinavia, in the latter regions including a 80-year linear trend of 1-1.5 mb (not shown). Considering that in the long-term mean the fringe of the Azores high-pressure system reaches Eastern Europe (not shown), the pattern can be interpreted to reflect summers with less pronounced subsidence over the Azores, but with the Azores high extending further than normal into the continent, thus leading to predominantly stable, warm weather conditions over Central Europe. An alternative explanation could however also be, that the SLP-subpattern represents a weak circulation induced by anomalously high temperatures over Central and Southern Europe.

Consistent with both interpretations, the first canonical mode predicts for Bern positive temperature and relative sunshine duration anomalies and a smaller probability for precipitation events ≥ 1mm (Fig. 6c, black bars). Interpreted with opposite signs, the first canonical mode describes summers with a higher than normal SLP over the Azores, but a corresponding low SLP over Europe, denoting that the continent is more frequently exposed to intrusions of cold air from west/north-west. This results in anomalously low temperatures at Bern, as well as over large areas south-east of the anomalously low SLP.

The second mode described mainly changes in the precipitation-related variables (cf. Fig. 6d, grey bars): similar to winter, higher than normal SLP centred over Britain (Fig. 6b, left) denotes summers with generally weaker westerlies and reduced advection of maritime air into Central Europe, whereas the associated intensified north-westerly flow implies negative near-surface temperature anomalies over Eastern Europe (Fig. 6b, right). In Bern, precipitation-related variables show negative deviations; mean daily temperature amplitudes as well as relative sunshine durations are above their long-term means; and, possibly due to reduced thunderstorm activity, the less pronounced zonal flow leads to negative deviations from summer mean wind speeds (Fig. 6c, grey bars). Clearly, since summer weather in Central Europe is mainly influenced by smaller-scale convective processes, the second canonical mode describes but a relatively small part of the interannual variability of the above mentioned variables (see also model verification below). Nonetheless, this mode can be interpreted to quantify for Bern the effects resulting from fluctuations in the intensity of the European summer monsoon (SCHüEPP & SCHIRMER, 1977).
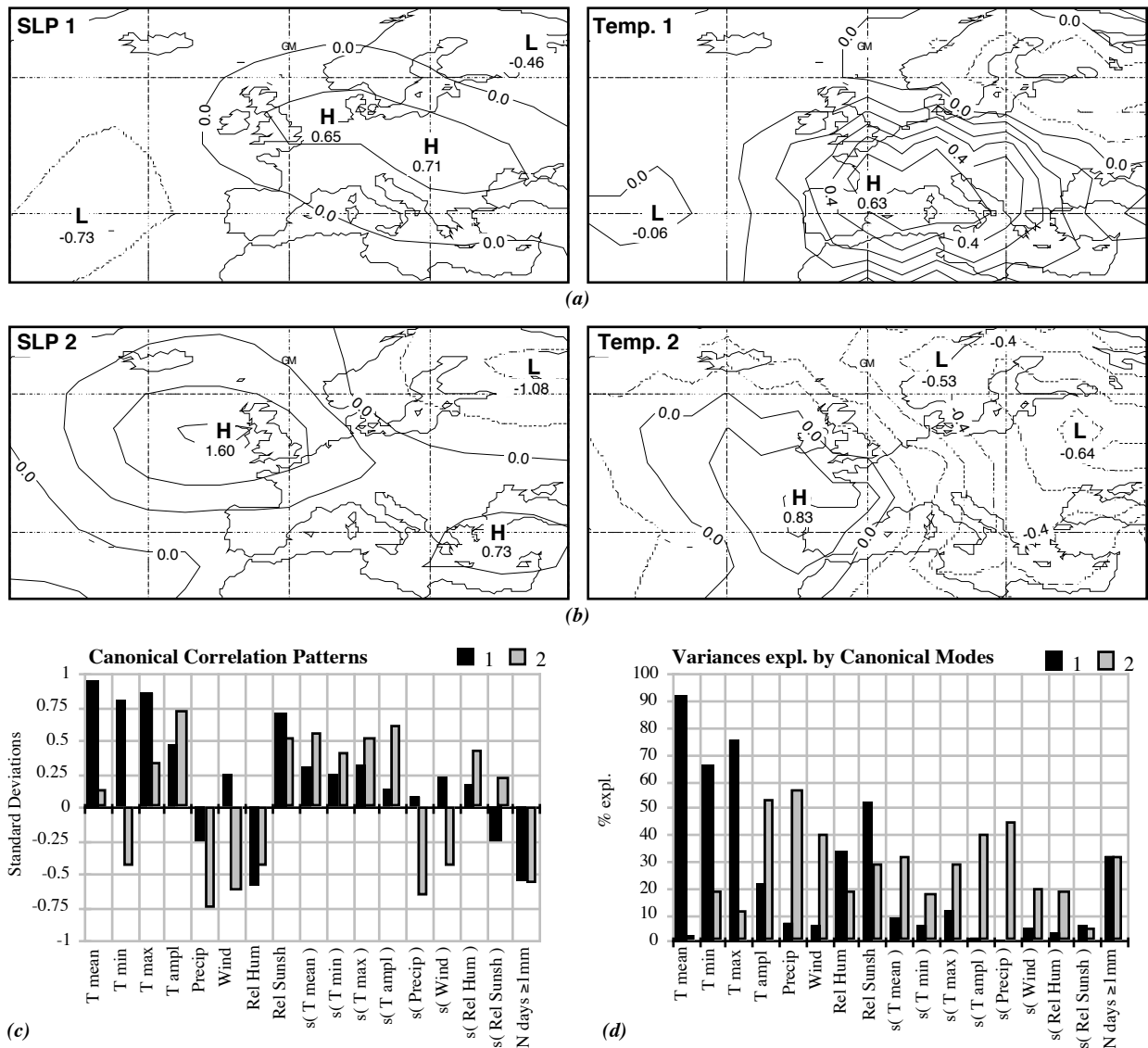
Fig. 6: CCA model for Bern in summer. (a) first, (b) second canonical pattern for the predictors. *Left* sides of (a) and (b): SLP subpatterns, contour-interval 0.5 mb. *Right* sides: near-surface temperature subpatterns, contour-interval: 0.1°C. (c) canonical patterns, (d) explained variances for the local weather statistics. The first 4 predictor EOFs and the first 4 weather statistics EOFs were used, explaining approx. 75% and 77% of the respective total variances. Correlations between time coefficients are 0.89 for the first and 0.75 for the second mode.

3.2 Model verification

For all five variants of SLP/near-surface temperature predictor data sets we determined per season and location according to Eq. 4 the respective best-performing 84 from 169 fitted CCA models. For each set of 84 CCA models, the models' capabilities to predict the individual weather statistics were assessed by comparing the statistically reconstructed interannual variations of the local variables with the observations. For six main weather statistics we also analysed the resulting 80-year linear trends.

a) Interannual Variability

The skill of the CCA models with regard to the individual variables was measured by the proportions of variance explained ($100 \cdot r_i^2$, $i = 1..84$) in the verification period 1941-80. Under the assumption of a normal distribution, correlations above 0.31, i.e. skills above ca. 10%, suggest a statistically significant link to large-scale climate ($\alpha = 95\%$).

Fig. 7 shows that the skill of the CCA models may vary strongly, depending on the large-scale predictors, the season, location, and weather statistic considered.
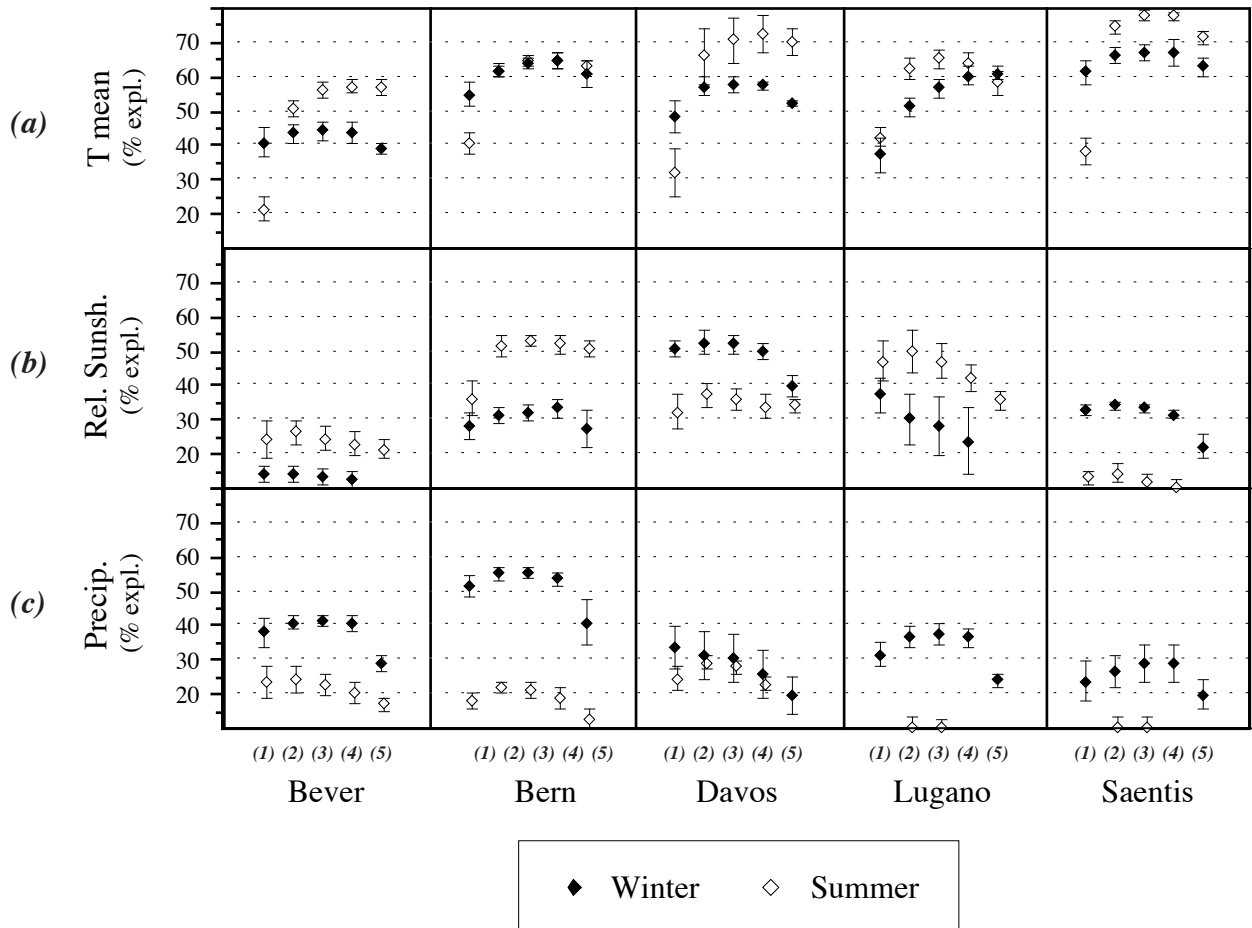

Fig. 7: Skill of the CCA models as a function of the predictor, season, location and variable considered. Shown are percentages of explained variances (=$100 \cdot r^2$) by the reconstruction of the weather statistics in the verification period 1941-80. Dots denote the mean variance explained by 84 selected CCA models, bars ±1 standard deviation. *From left to right* (repeated for each location): (1) predictors were SLP anomalies alone, (2) predictors were SLP- and near-surface temperature anomalies accounting for the total variance of the predictor data with the ratios 2:1, (3) 1:1, (4) 1:2, and (5) predictors were temperature anomalies alone.

Though no combination of predictors could be found which yielded optimal results for all cases, the combined use of SLP and near-surface temperature generally improved the skill of the procedure (predictor data set variants 2-4 in Fig. 7). On average over all locations and variables, the mean variances explained when SLP (near-surface temperature) alone was used, amounted to ca. 23% (21%) in winter and to 12% (18%) in summer. An optimum was reached when the two fields were combined with equal weights, such that an average skill of 25% in winter and 19% in summer was attained. Use of the two predictors with equal weights seemed therefore to be a

good compromise, which was maintained for the further discussion and for obtaining climatic change estimates from the GCM-experiments.

As can be seen from Fig. 8, the most dramatic improvement occurred for the summer, and for temperature-related variables. However, the situation remained, that most variables were better linked to the large-scale state of the atmosphere in winter than in summer.

In both seasons, better results were obtained at the three north alpine locations (Bern, Davos, Saentis) where, on average over all three locations and all variables, the mean skill of the CCA models amounted to 29% in winter and to 21% in summer. At the more southern locations (Bever, Lugano) on average only 20% (winter) and 17% (summer) were attained.
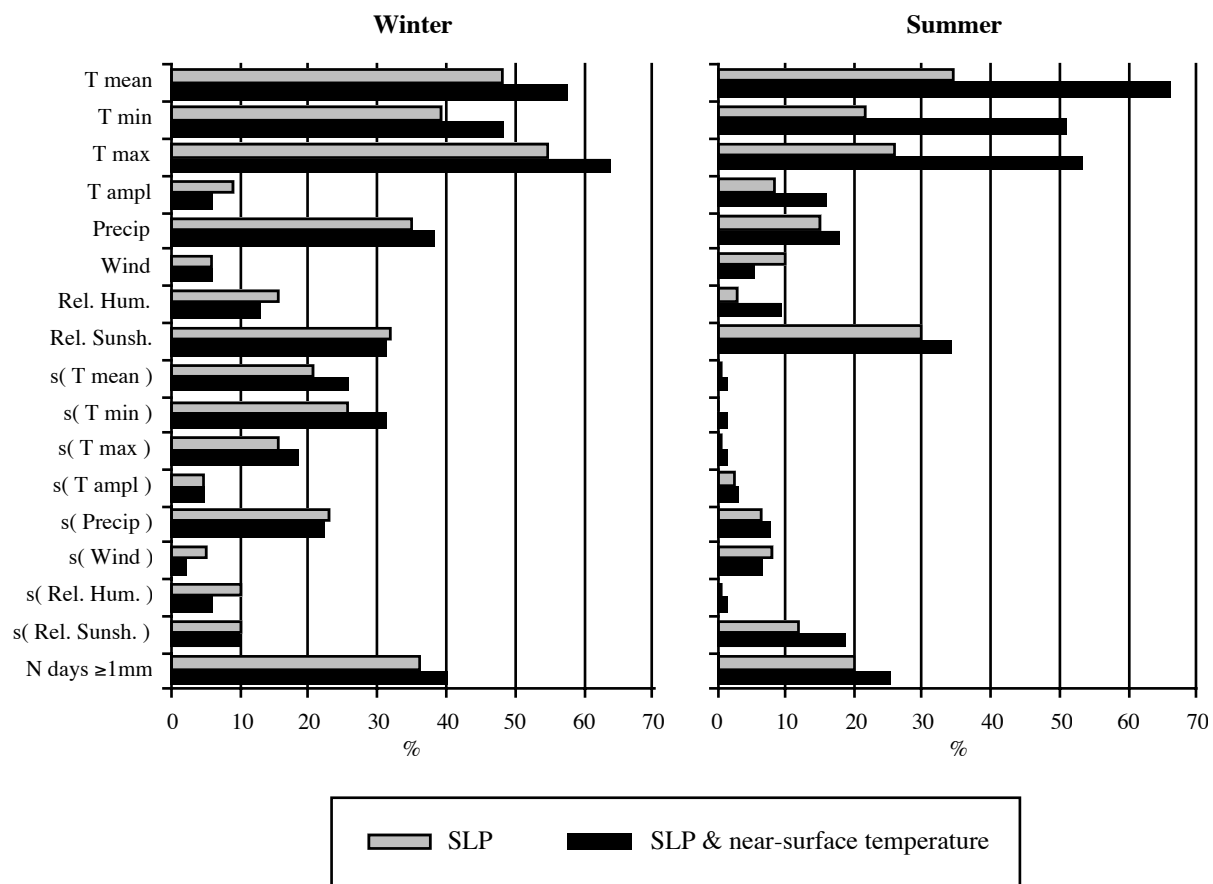

Fig. 8: Comparison of skills between the procedure proposed by VON STORCH *et al.* (1993) (grey bars) and the improved procedure (black bars). Shown are mean percentages of explained variances (=100·r^2) in the verification period 1941-80 from all five case-study locations and all 84 selected CCA models fitted per season and location.

Large differences were found between the individual variables (Fig. 8). Temperatures were generally better reproduced than precipitation-related variables, the latter being particularly poorly predicted in summer. For seasonal mean temperatures, mean skills from the respective 84 selected CCA-models were between 44% (Bever) and 67% (Saentis) in winter, and 56% (Bever) and 78% (Saentis) in summer (cf. Fig. 7a, data set variant 3). Mean daily temperature minima which, except for Bern (not shown), were at all locations better reproduced in summer than in winter, were predicted with mean skills ranging from 30% (Lugano) to 64% (Saentis) in winter, and from 36% (Lugano) to 73% (Saentis) in summer. Mean daily maximum temperatures were also generally well predicted, with skills ranging in winter from 59% (Bever) to 69% (Bern), and in summer from 33% (Lugano) to 74% (Saentis). Mean daily temperature amplitudes were not well reproduced at any location in winter, but in summer skills of 19%, 24% and 32% were

attained at Bever, Saentis, and Bern, respectively. For precipitation, between 29% (Saentis) and 55% (Bern) were reached in winter, and between 10% (Lugano, Saentis) and 28% (Davos) in summer (cf. Fig. 7c). Relative sunshine durations, which directly depend on cloud amount, were also less well reproduced; exceptions were however Davos (52%) in winter, and Bern (53%) and Lugano (47%) in summer (cf. Fig. 7b). Skills for the numbers of days with precipitation above 1mm ranged from 29% (Davos) to 56% (Bern) in winter, and from 4% (Bever), followed by 18% (Davos), 30% (Saentis), 36% (Lugano), to 42% (Bern) in summer. Not well predicted were seasonal mean wind speeds; the highest skills were attained in winter at Davos (18%) and in summer at Saentis (15%). Mean relative humidities were only well reproduced at Saentis in winter (43%), whereas in summer at no location more than 15% were reached. Within-season standard deviations of daily mean, minimum and
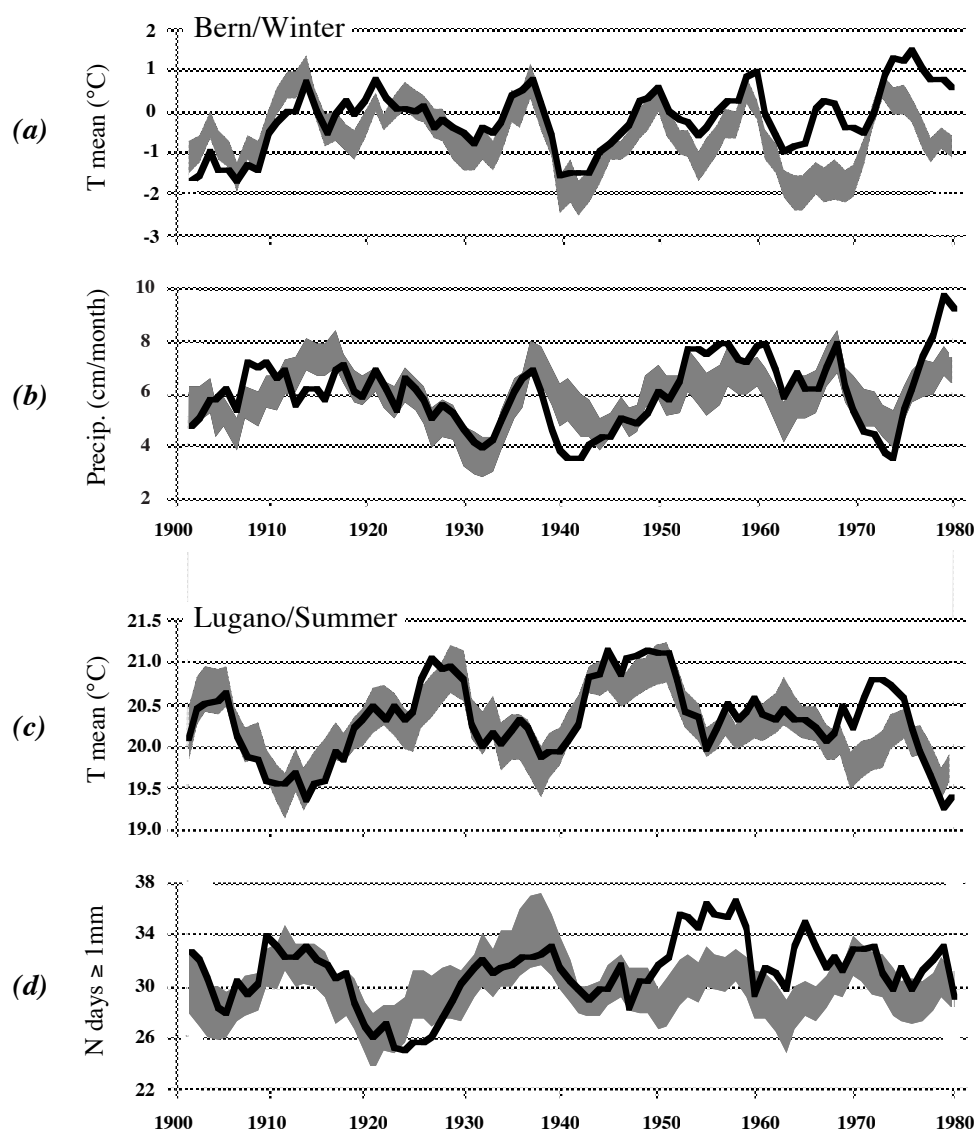
Fig. 9: Comparison of statistically reconstructed time series of local weather statistics with observations (five-year running means). Solid lines: observations 1901-80. Grey areas contain 90% of the reconstructed values from 84 selected CCA models fitted separately for each season and location for the years 1901-40 using a combined SLP/near-surface temperature predictor data set (weights 1:1). Explained variances by the average time series (not shown) of the 84 CCA models in the verification period 1941-80 were (a) 64%, (b) 55%, (c) 65%, (d) 36%.

maximum temperatures were predicted in winter with skills between 20% and 45%; an exception was Lugano, where skills for all three parameters were below 10%, as was the case for all locations in summer. For the within-season standard deviations of daily precipitation totals, skills above 20% were reached at Bever (24%), Bern (29%), and Lugano (39%) in winter, but, again, at no location in summer. From all remaining within-season standard deviations, a skill above ca. 20% was reached only for relative sunshine durations at Bern (21%) and Davos (20%) in winter, and at Bever (19%) and Lugano (52%) in summer.

In Fig. 9, five-year running-means of observed (thick lines) and reconstructed (grey areas) time series of weather statistics are compared, showing a generally coherent behavior between the pairs of curves. The better reproduction of temperatures (Figs. 9a,c) in contrast to precipitation related variables (Figs. 9b,d) also becomes visible in the different widths of the grey areas, i.e. the uncertainties resulting from different choices in the numbers of EOFs used to fit the statistical models.

One main reason for the differences in the predictability of the local variables between the different locations, seasons and variables is certainly that our approach describes only the proportion of the interannual variability of a weather statistic which is controlled by fluctuations of large-scale SLP and near-surface temperature. Differences may thus result from seasonally (winter vs. summer) or regionally (northern vs. southern Alps) varying intensities of smaller-scale convective activity, as well as from different combinations of local factors such as topography, vegetation, and soil characteristics. In particular, the latter may regionally modify local wind systems, snow cover, or energy exchange with the atmosphere, thus uncoupling the variability of individual weather elements from the large-scale circulation. For example, seasonal mean minimum temperatures, which depend on smaller-scale thermal inversions and cold air drainage, were generally less well reconstructed than the seasonal mean and mean maximum temperatures. As could be expected, this was found to be particularly the case for the four valley locations, and for the winter season.

It should be noted that the inclusion of 17, not equally well cross-correlated variables within the same CCA model tended to worsen the prediction of individual variables to the benefit of the ensemble. This is because – in spite of the standardisation of all predictands to unit standard deviation (Fig. 3) – the relative importance of individual variables is implicitly influenced by typical correlation structures found in the predictand data sets, e.g. a clustering of temperature- or precipitation-related variables. Possibly, due to an alternative choice or weighting of the predictands, the modest performance obtained for e.g. mean relative humidities and wind speeds could be improved.

b) Long-term Linear Trends

The observed and by means of CCA reconstructed 1901-80 linear trends of six main weather statistics are summarised in Table 2.

Seasonal daily mean, mean minimum and mean maximum temperatures underwent in winter an upward trend at all five stations. The CCA models failed uniformly to reproduce even the signs of these trends and indicated a decrease of temperature since the beginning of this century. For the interannual variations however, the similarity between reconstructed time series and the in-situ observations was much better (Fig. 9a). A similar finding was reported by WERNER & VON STORCH (1993).

CCA specified a net cooling because of a large-scale trend of SLP (Fig. 10a), whereas the spatially more inhomogeneous trend in the VINNIKOV temperature data (Fig. 10b) did not much affect the reconstruction of the temperature trends (s.a. Eq. 1'). The reality of the long-term SLP trend was documented by VON STORCH et al. (1993), who found a consistent signal in both ship-of-opportunity observations of SLP and in in-situ precipitation records on the Iberian Peninsula. When only SLP was used for CCA, the discrepancy between the CCA models and the local observations was increased (mean and standard deviation of trend from 84 selected

CCA models for winter mean temperature in Bern: -1.21±0.28 °C per 80 years). The differences between the 80-year trends also remained, if the 1941-80 interval was used to fit the CCA models.

Seasonal Statistics		Bever		Bern		Davos		Lugano		Saentis	
		obs.	*rec.*	*obs.*	*rec.*	*obs.*	*rec.*	*obs.*	*rec.*	*obs.*	*rec.*
Winter	Tmean (°C)	0.78	-0.51	1.34*	-0.49	1.75*	-0.53	1.17*	-0.47	0.63	-0.99
	Tmin (°C)	1.16	-0.34	2.36*	-0.43	2.64*	-0.44	2*	-0.46	0.52	-1.03
	Tmax (°C)	0.60	-0.56	0.36	-0.76	0.77	-0.59	0.44	-0.77	0.82	-0.98
	Rel.Sunsh. (%)	-11.6*	-2.1	-3.1	-3.4	-6.2	-4.2	-6.0	-4.5	-0.9	-2.2
	Precip. (% of LTM)	-20.9	7.4	16.3	6.6	12.2	0.5	28.4	18.1	-47.4*	-2.7
	Ndays≥1mm(% of LTM)	-9.3	8.0	2.6	3.6	5.2	6.2	27.8	20.9	-9.4	3.4
Summer	Tmean (°C)	-0.01	0.25	0.50	0.02	0.05	0.04	0.22	-0.09	0.69	0.16
	Tmin (°C)	0.27	0.21	1.24*	0.18	1.22*	0.13	2.13*	0.03	0.61	0.19
	Tmax (°C)	-0.58	0.60	-0.25	-0.12	-0.21	-0.06	-2.21*	-0.23	0.80	0.17
	Rel.Sunsh. (%)	-5.1*	-1.6	-6.6*	-0.6	-7.3*	-1.2	-10.3*	-0.7	6.0*	0.2
	Precip. (% of LTM)	7.1	5.8	1.1	-0.8	-1.7	-1.2	-5.4	4.7	-16.2	-4.9
	Ndays≥1mm(% of LTM)	0.9	0.5	-3.1	-0.6	-0.3	-1.2	9.7	1.4	-0.1	-3.3

Table 2:   Observed (*obs.*) and from 84 selected CCA-models mean reconstructed (*rec.*) linear trends of weather statistics in the period 1901-80. The CCA-models were fitted for the years 1901-40 to a combined SLP/near-surface temperature predictor data set (weights 1:1). Quantities are given in respective units per 80 years; asterisks denote significance of trends on the 95% level (F-test, Ho = slope of the linear regression of the respective time series from time equals zero; given for observations only). LTM = long-term (1901-80) mean.

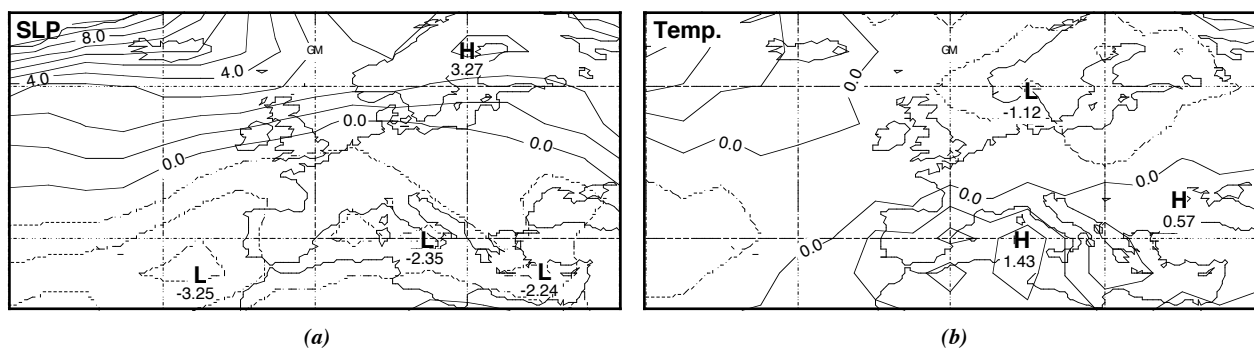(a)   (b)

Fig. 10: 1901-80 linear trends in the used data sets for (a) winter mean SLP (contour interval 1 mb) and (b) winter mean near-surface temperature (contour interval 0.5 °C).

There are several candidates that may account for part or all of the discrepancy:

First, the effect of the systematically changing pressure field on the Swiss temperature must have been counteracted by another large-scale feature, presumably representing the thermal structure of the troposphere. One possibility is, that, e.g. due to the use of changing reference intervals, a real trend in near-surface temperature is not correctly represented in the VINNIKOV data set. Preliminary calculations with the JONES-data set (JONES & BRIFFA, 1992; BRIFFA & JONES, 1993) actually yielded less negative 80 year-trends for winter mean temperatures, however by only 0.1-0.3 °C. An alternative explanation could thus be a trend in a large-scale parameter not included in our analysis, e.g. 500 mb geopotential height. Due to the lack of data in the first half of this century this hypothesis could however not be tested.

A second reason could be that the statistical link between the local temperatures and the large-scale circulation has changed with time. For example, systematic changes in the frequencies of short-lived weather systems which have a strong effect on the local temperatures may not be adequately represented in the seasonal mean fields. Possibly, the linear CCA models may also have failed to capture any non-linear effects.

Finally, it should be noted that the positive trends are significant only for the seasonal mean and mean minimum temperatures at the three urban stations, whereas the two rural stations Bever and Saentis show much smaller trends (Table 2). From Fig. 9a it becomes obvious that the CCA models failed to reproduce the trend not only in the last 40 years of the verification interval but also in the first 40 years of the analysis interval. We speculate, that the positive local trends at the urban stations are overestimated due to the urban heat island effect and the increasing air pollution.

In summer, the discrepancy between the indirectly derived and the in-situ trends of the three temperature parameters was considerably smaller than in winter. Only the trends of the mean minimum temperatures at the three urban stations were not reproduced. We suggest that these in-situ records are certainly contaminated by a significant urbanisation effect. Another major difference happened at Lugano, where the in-situ observations of seasonal mean daily temperature maxima indicate a net cooling of -2.2 °C, whereas the large-scale field specified a small cooling of only -0.2 °C.

For relative sunshine in winter the statistical models were more successful in reproducing the sign of the trends, even if the absolute values deviated somewhat. The significant reduction of relative sunshine obtained for Bever, as well as its bad reproduction by the CCA models (Fig. 7b), is most probably because measurements for this location were taken from the climate station of St. Mortis 6.9 km apart, which also has been often displaced.

Trends in summer mean relative sunshine durations were generally underestimated by CCA, but the signs were in all five cases correct. The largest deviations were found for Lugano, where relative sunshine decreased during 1901-80 by more than 10%, whereas the CCA models estimated a reduction by only 0.7%. Again, this discrepancy could be caused by displacements of the climate station (H. BANTLE, SMA, pers. comm.) or by increased air pollution (s.a. GENSLER, 1978, p. 9).

Trends of daily mean precipitation and of numbers of days with precipitation exceeding 1 mm were mostly reproduced with an error remaining within 10% of the respective 1901-80 long-term means. At Bever, observed (-21%) and reconstructed (+7.4%) winter precipitation trends were not consistent, but both numbers are small compared to the 1901-80 standard deviation which amounts to ca. 49% of the long-term mean. The significant trend found for mean winter precipitation in Saentis, which was also not well reconstructed by means of CCA, is doubtful, since precipitation may not be reliably measured at this peak location.

3.3 Downscaling of GCM-Simulated Climatic Changes

GCM-simulated predictors for the climatic change experiments performed with the ECHAM1/LSG-GCM were derived as deviations from the mean SLP and near-surface temperature fields simulated in the first 40 years of the "control" run. The "control" run shows a drift in the globally and annually averaged near-surface temperature of less than -0.4 °C in 100 years, which may be attributed to low-frequency variability of the model. In the DCO2-experiment, after one century temperature has increased by 1.7 °C. In the SCNA-experiment, global mean temperature rises during the first 40 years by moderate 0.5 °C, which is likely an under-estimation due to the "Cold Start"-problem (see HASSELMANN *et al.*, 1992). The rate of temperature growth increases then to 0.35 °C per decade, such that by the year 2085, and under greenhouse gas concentrations of ca 1150 ppm equivalent CO_2, global warming reaches 2.6 °C. This result lies between the lowest and best estimates of approx. 2 °C and 3 °C, respectively, given for the same future timepoint by HOUGHTON *et al.* (1990).
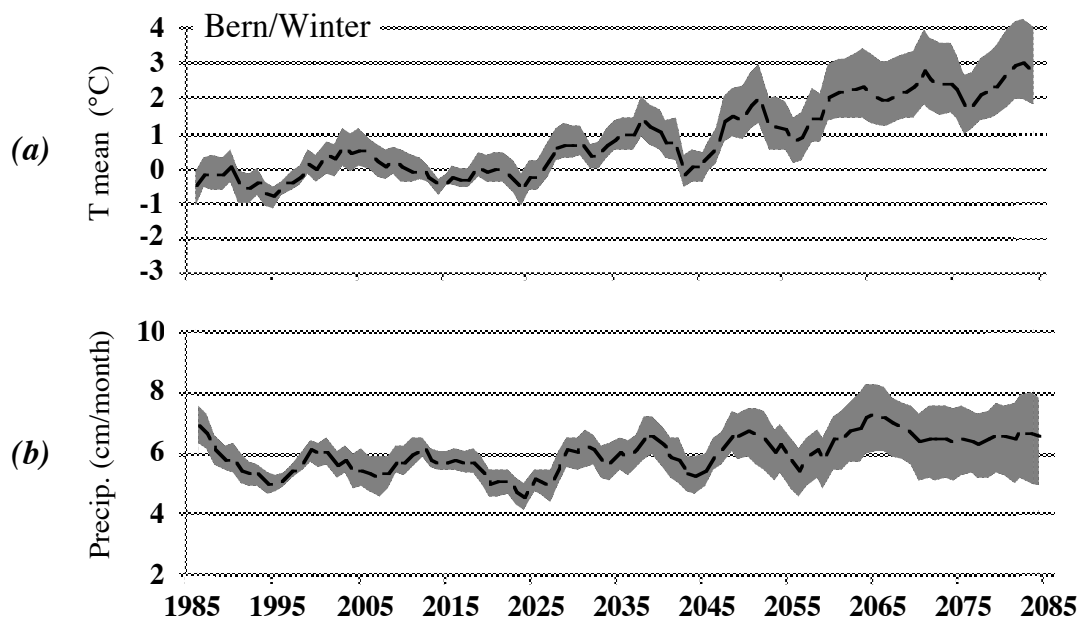

Fig. 11: Climatic change scenario for Bern (five-year running means). Changes in the local variables were statistically downscaled from large-scale SLP and near-surface temperature anomalies simulated in the "IPCC Scenario A"-experiment performed with the ECHAM1/LSG-GCM. Dashed lines: mean responses of 84 selected CCA models using different numbers of EOFs. Grey areas contain 90% of the CCA model estimates.

Fig. 11 shows time-dependent changes in the temperature and precipitation statistics of Bern downscaled from the SLP and near-surface temperature anomaly fields of the 100-year SCNA-experiment. The range of values predicted by the different CCA models using different numbers of EOFs typically increases with time, i.e. with the magnitude of large-scale climatic change. This is because differences in the regression coefficients of Eq. 3 become increasingly effective, the more the predictors deviate from the mean state used for CCA model estimation.

In Figs. 12 and 13 projected changes in seasonal temperature and precipitation parameters are compared between locations. The obtained regional differentiation is in strong contrast to the homogeneous changes specified at single GCM-gridpoints on a spatial scale of several 10^2 km (cf. Fig. 1). During the last decade of the SCNA-experiment, the projected temperature deviations differ between locations by as much as 1.8 °C in winter and 2.0 °C in summer. Similarly pronounced differences occurred for most other variables as well (Fig. 13).

As can be seen from Fig. 12, the DCO2- and the SCNA-experiment yielded similar patterns of change between the different locations. Since this was not only the case for temperature (s.a. Table 3 below), in the following we will focus on the last decade of the SCNA-experiment, where the most pronounced changes occurred. Further, since for some variables the downscaled changes strongly depended on the data used for CCA model estimation (Fig. 13), the mean responses of CCA models fitted in the period 1901-40, as well as in the complementary period 1941-80 will be considered.
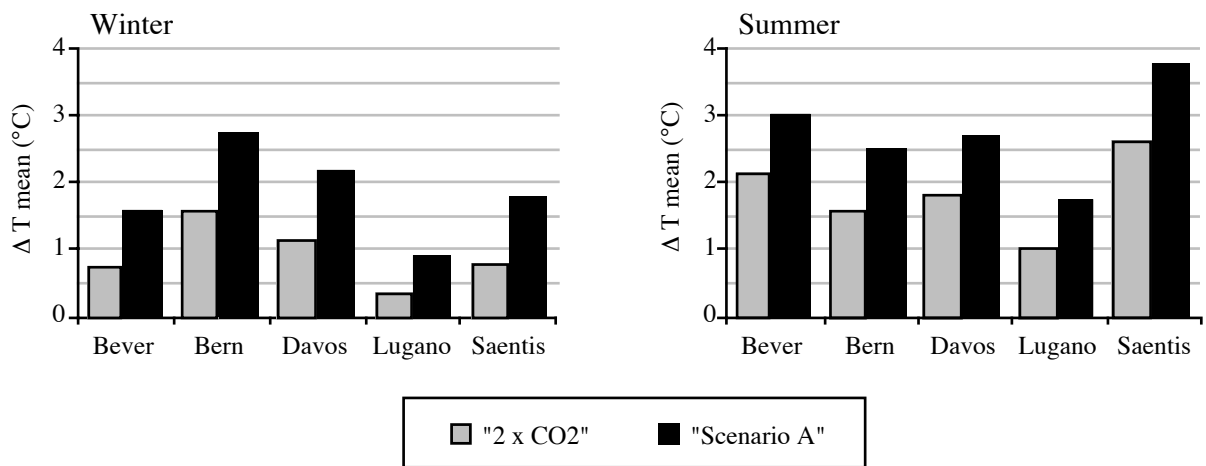
Fig. 12: Statistically downscaled changes in seasonal mean temperatures for the last 20 years of the "2xCO2"- experiment and for the last 10 years of the "IPCC Scenario A"-experiment. Shown are the mean changes obtained from 84 selected CCA models fitted in the period 1901-40 separately for each season and location. Changes are given relative to the 1901-40 means.
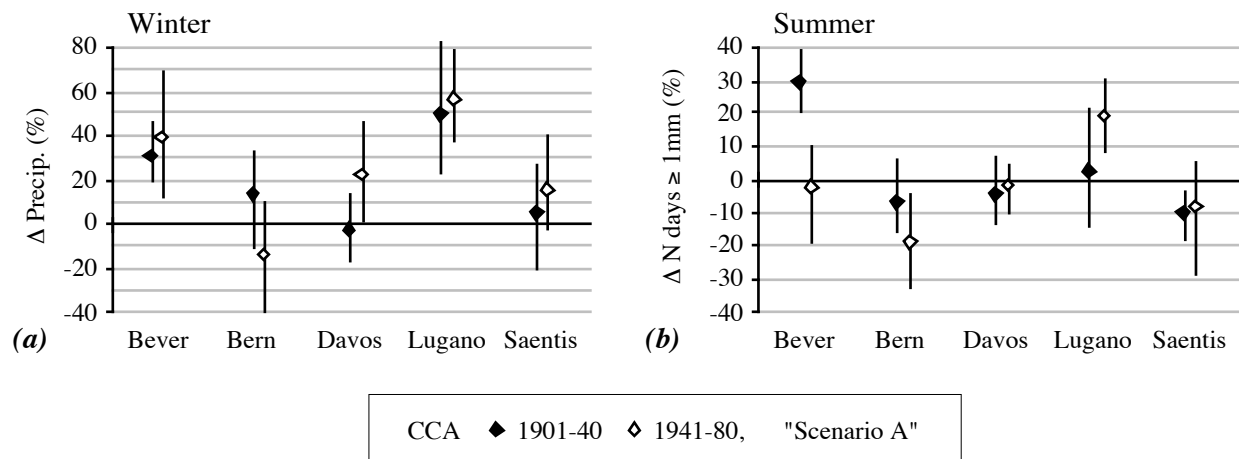
Fig. 13: Statistically downscaled changes in (a) winter precipitation totals and (b) summer probabilities of days with precipitation ≥ 1mm for the last 10 years of the "IPCC Scenario A"-experiment. The CCA models were fitted in the periods 1901-40 (black dots) and 1941-80 (white dots), respectively. Dots indicate mean changes obtained from a set of 84 selected CCA models fitted separately for each period, season and location, bars denote the empirical intervals containing 90% of the respective CCA model responses. Changes are given relative to the 1901-80 means.

Seasonal Statistics	Loca-tion	Winter								Summer							
		1901-80		DCO2			SCNA			1901-80		DCO2			SCNA		
		μ	σ	low	b.e.	high	low	b.e.	high	μ	σ	low	b.e.	high	low	b.e.	high
Tmean	Bever	-8.26	1.44	0.15	**0.62**	1.13	0.46	**1.29**	2.14	10.68	0.84	1.41	**2.00**	2.73	1.98	**2.80**	3.75
	Bern	-0.21	1.56	0.72	**1.25**	2.10	1.64	**2.31**	3.51	16.82	0.98	1.12	**1.72**	2.70	1.93	**2.52**	3.71
	Davos	-5.58	1.54	0.48	**0.93**	1.38	1.04	**1.82**	2.51	11.37	0.89	0.82	**1.74**	2.39	1.39	**2.53**	3.48
	Lugano	2.92	0.97	-0.21	**0.45**	0.95	0.15	**1.03**	1.64	20.30	0.80	0.47	**1.24**	2.13	1.03	**1.95**	3.01
	Saentis	-8.17	1.37	0.36	**0.88**	1.46	1.24	**1.86**	2.72	4.20	0.97	1.73	**2.21**	2.84	2.35	**3.15**	4.13
Tmin	Bever	-14.56	1.69	0.09	**1.05**	2.27	0.29	**1.83**	3.62	4.07	0.66	1.11	**1.64**	2.60	1.48	**2.24**	3.31
	Bern	-3.01	1.71	0.63	**1.40**	2.06	1.57	**2.51**	3.46	11.99	0.82	1.12	**1.85**	2.57	1.47	**2.53**	3.27
	Davos	-9.96	1.70	0.64	**1.22**	2.03	1.18	**2.14**	3.40	5.93	0.84	0.18	**1.74**	2.85	0.58	**2.47**	4.15
	Lugano	-0.60	1.23	-0.23	**0.45**	1.21	0.35	**1.12**	1.96	14.85	0.99	-0.13	**0.77**	1.62	0.30	**1.22**	2.04
	Saentis	-10.64	1.39	0.45	**0.93**	1.43	1.33	**1.91**	2.60	1.76	0.89	1.48	**1.93**	2.46	1.99	**2.70**	3.51
Tmax	Bever	-1.87	1.29	0.19	**0.54**	0.93	0.64	**1.17**	1.75	17.63	1.43	1.90	**3.28**	4.62	2.83	**4.59**	6.29
	Bern	2.95	1.60	0.46	**0.93**	1.61	1.37	**1.93**	2.94	22.10	1.26	0.94	**1.82**	3.18	1.79	**2.75**	4.51
	Davos	-0.61	1.34	0.35	**0.77**	1.10	0.94	**1.61**	2.03	16.56	1.07	1.15	**1.78**	2.39	1.87	**2.63**	3.50
	Lugano	7.29	1.13	-0.59	**0.36**	1.47	-0.33	**0.92**	2.56	26.76	1.34	0.48	**2.19**	4.39	0.90	**3.29**	6.30
	Saentis	-5.36	1.38	0.26	**0.80**	1.44	1.08	**1.73**	2.68	7.13	1.15	2.12	**2.67**	3.38	2.88	**3.82**	4.94
Rel. Sunsh.	Bever	42.28	9.28	-15.2	**2.5**	12.5	-19.6	**4.7**	27.5	50.84	5.77	-9.3	**10.6**	41.4	-10.7	**22.0**	67.4
	Bern	24.13	5.60	-18.0	**-1.7**	8.9	-19.2	**1.8**	14.1	51.99	6.71	0.8	**9.6**	19.6	5.6	**16.4**	30.0
	Davos	49.93	8.40	-10.2	**-3.6**	2.0	-12.0	**-3.1**	6.2	49.37	5.91	-7.4	**3.6**	14.1	-4.1	**8.5**	20.4
	Lugano	52.61	8.44	-11.7	**-4.1**	0.8	-16.1	**-4.5**	4.4	63.88	5.77	1.0	**6.4**	13.4	2.9	**11.4**	21.9
	Saentis	38.19	8.87	-28.2	**-4.3**	24.2	-20.4	**8.1**	66.0	34.95	5.30	-0.2	**54.2**	162.1	4.8	**82.5**	223.9
Precip.	Bever	4.53	2.21	-5.1	**17.5**	35.4	4.4	**34.0**	56.9	9.90	2.42	-2.6	**25.7**	55.9	-6.9	**30.2**	71.3
	Bern	5.98	2.60	-23.5	**-1.3**	14.3	-38.3	**-1.0**	27.0	11.48	3.06	-25.4	**6.9**	39.4	-36.5	**4.1**	44.8
	Davos	6.77	2.84	-16.2	**5.0**	32.0	-21.2	**9.7**	52.7	12.89	2.37	-5.3	**8.9**	18.6	-12.0	**7.3**	20.9
	Lugano	7.40	4.03	2.7	**28.9**	57.1	17.5	**53.0**	88.5	18.07	5.50	1.1	**22.9**	52.4	-3.6	**22.9**	59.2
	Saentis	20.71	9.82	-18.7	**6.3**	42.1	-15.9	**9.1**	43.9	27.86	6.91	-60.7	**-27.5**	1.6	-89.5	**-42.5**	-0.5
Ndays≥1mm	Bever	21.64	6.68	-4.3	**7.2**	18.7	-0.8	**14.7**	31.0	33.48	5.07	-11.9	**12.2**	32.5	-20.2	**13.5**	40.5
	Bern	28.51	8.64	-22.2	**-2.3**	14.8	-34.8	**-3.0**	24.3	35.08	7.33	-23.3	**-6.0**	11.8	-33.8	**-13.1**	8.5
	Davos	26.31	6.63	-11.4	**0.4**	12.9	-18.3	**1.2**	20.7	42.31	5.37	-8.2	**-0.2**	8.0	-13.4	**-3.5**	7.0
	Lugano	18.69	7.24	0.2	**16.7**	31.2	9.2	**27.5**	49.1	31.06	5.83	-8.5	**11.8**	31.0	-17.0	**10.8**	34.6
	Saentis	41.81	9.60	-10.5	**0.7**	13.8	-12.4	**1.8**	18.6	49.81	6.87	-20.6	**-4.9**	7.1	-28.9	**-9.6**	5.1

Table 3: Projected deviations of weather statistics from their respective 1901-80 long-term means (μ) for the last 20 years of the "2xCO2"-experiment (DCO2) and for the last 10 years of the "IPCC Scenario A"-experiment (SCNA). σ = 1901-80 observed standard deviations of the weather statistics; b.e. = "best estimate" changes, i.e. mean deviations obtained from 2·84 = 168 selected CCA models estimated for the years 1901-40, respectively 1941-80 using a combined SLP/near-surface temperature predictor data set (weights 1:1); low/high = lower and upper limits of empirical intervals containing the responses of 151 (=90% of 168) CCA models. 1901-80 means and standard deviations are given for the temperature parameters in °C, for relative sunshine duration in %, and for precipitation in cm/month. Deviations are given for temperatures in °C and for all other variables in % of the respective 1901-80 means.

The results for six main variables are summarised in Table 3. For seasonal mean temperatures, the "best estimates" – i.e. the mean changes from all used CCA models per season and location – amounted on average over the three northern locations Bern, Davos, and Saentis (the two more southern locations Bever and Lugano) to 2.0 °C (1.2 °C) in winter, and to 2.4 °C (2.7 °C) in summer. Winter mean daily temperature extrema showed similar spatial patterns of change as the winter temperature means: winter mean daily minimum temperatures were found to rise at the northern (southern) slope of the Alps by on average 2.2 °C (1.5 °C), whereas for the maxima moderate changes by 1.8 °C (1.0 °C) occurred. Warming was very differently distributed in summer, where a substantial increase by 3.1 °C (3.9 °C) was obtained for the temperature maxima, as opposed to only 2.6 °C (1.7 °C) for the temperature minima. Projected changes in relative sunshine durations were for winter generally small, whereas in summer changes of +36% were specified at the northern, and +17% and the southern slope of the Alps. Winter precipitation totals changed by only ca. +6% at the northern, but increased dramatically by 34% (Bever) and 53% (Lugano) at the more southern locations (s.a. Fig. 13a). Summer precipitation was found to increase at all locations by 4%-30%, except for Saentis, where a strong decrease by 42% was specified; the strongest increase occurred again at the southern slope of the Alps (average 26%). Winter probabilities of wet days did not change much at the three northern loca-

tions, whereas at Bever increases by 15% and at Lugano by 28% were obtained; summer probabilities of wet days were found to change at the three northern locations by -3% to -13%, and, again, to increase at the two more southern locations by on average ca. 12% (s.a. Fig. 13b).

The following "best estimates" were obtained for the weather statistics not considered in Table 3: Seasonal mean daily temperature amplitudes decreased in winter quite uniformly by on average -0.4 °C; in summer they increased at the three northern locations by on average 0.5 °C, and at the two southern locations by 2.2 °C. Winter daily mean wind speeds were found to decrease at Bever by 48% and at Davos by 40%, and at Lugano to increase by 9% of the respective long-term mean; in summer, mean wind speeds decreased again at Bever (-75%) and Davos (-64%), but increased by 35% at Bern and 61% at Lugano. Seasonal mean relative humidities did not change much in both seasons at all locations, except for Saentis in summer (-15%). Within-season standard deviations of daily mean, minimum and maximum temperatures decreased systematically at all locations, on average by 21%, 21% and 18% in winter and by 11%, 10% and 7% in summer, respectively. Within-season standard deviations of daily temperature amplitudes were reduced in winter by ca. 10%, whereas in summer less coherent changes between locations, in the order of ±10%, were obtained. Within-season standard deviations of daily precipitation totals increased in winter at Bever and Lugano by 40% and 46%, respectively, and in summer by 5%-24% at all locations, except for Saentis, where a reduction by 41% occurred. Within-season standard deviations of daily relative sunshine durations changed in winter only at Saentis (+10%), whereas in summer, increases at Saentis (+74%) as well as at Bever (+10%), and decreases by 5% to 10% at the remaining locations were specified.

The procedure yielded not only a regionally differentiated, but also an internally consistent picture of possible climatic change. Note that plausible changes were even obtained for several variables which were not well predicted in the model verification phase. In some cases however, e.g. for summer precipitation and mean relative sunshine duration at Saentis, the CCA models did not yield sensible results. Possible reasons could be that the linearity assumption (Eq. 3) was violated, or that inconsistencies in the local data sets were amplified under the given large-scale climatic change. All in all, winter climate was specified to be milder and wetter than under present conditions. This suggests an increased probability for night-time cloud cover, which is consistently mirrored in a stronger rise of the minimum as compared to the maximum temperatures, a general decrease of mean daily temperature amplitudes, and a smaller within-winter temperature variability. The summer was specified to become generally hotter and wetter; hereby, strong increases in relative sunshine durations, mean daily maximum temperatures and temperature amplitudes suggested increased irradiation and surface heating. The increases in summer precipitation could thus correspond to stronger convective activity, or to more intense intrusions of maritime air compensating a more pronounced ocean-continent temperature contrast also found in the GCM-simulated temperature field. In both seasons, the precipitation increases consistently tended to go with increased within-season variabilities of daily precipitation totals, and increased probabilities of wet days.

It should be noted that the large-scale signals underlying the responses of all weather statistics (Eq. 1') were found in both seasons and for all locations to be mainly determined by the rising near-surface temperature. In particular, the projected changes depended strongly on the inclusion of near-surface temperature as a large-scale predictor. For example, when SLP was used as the only predictor in winter, anomalously high SLP between 35° N and 50° N in the final decade of the SCNA-experiment implied precipitation decreases by 4% to 12% in Bever, Bern and Lugano, and positive changes of a few percent in Saentis and Davos. Quite differently, in Fig. 12a are shown precipitation increases which, since they include the information of the temperature field, can be interpreted to be a consequence of the higher moisture content of the air advected towards the Alps, counterbalancing the effect of slightly weakened westerlies. It is possible, that inclusion of additional predictors which show similarly drastic changes as near-surface temperature in the GCM, e.g. mid-tropospheric pressure fields, could further modify our results.

The downscaled climatic changes strongly reflected the characteristics of the underlying GCM-simulation. The DCO2- and the SCNA-experiment yielded qualitatively similar changes in local climates (Fig. 12, Table 3) because the GCM's large-scale responses for SLP (not shown) as well as for near-surface temperature (CUBASCH *et al.*, 1992) to the respective greenhouse-gas forcings show in both experiments quite similar large-scale patterns. In the case of the SCNA-experiment, the small changes projected for the first 50 years of the scenario period (Fig. 11) reflect the delayed global mean temperature response of the ECHAM1/LSG-GCM. Further, the GCM-downscaled year-to-year fluctuations of the weather statistics were generally smaller than under present climate (Fig. 9 vs. Fig. 11). This is due to a systematic underestimation of the interannual variability of seasonal mean SLP by the GCM which occurs in the "control" run, as well as in the first decades of the SCNA-experiment for both seasons considered (not shown). A possible reason for this could be the underestimation of mid-latitude cyclonic activity resulting from the model's low spatial resolution (cf. CUBASCH *et al.*, 1992). Finally, it should be noted that the smallest warming occurred for both seasons at the southern slope of the Alps (Lugano). This is most likely because temperatures at the north alpine locations (Bern, Davos and Saentis) and at the more eastwardly located Bever are more strongly determined by advection from higher latitudes and North-Eastern Europe, which are the regions where the largest warming takes place in the GCM.

4. CONCLUSIONS

From our case studies at five representative locations in the Alps we conclude:

(1) It is possible to establish plausible statistical relationships which allow to link the large-scale climatic changes as produced by GCMs to local ecosystem model inputs, even in a complex orography like the Alps. The obtained results were meaningful for winter (DJF) as well as for summer (JJA). The statistical models quantified for each location the effects resulting from changes in major circulation patterns, e.g. from changes in the strengths of large-scale zonal or meridional flow or of subsidence, and from fluctuations in the associated large-scale near-surface temperature distributions.

(2) The strength of the statistical link to the large-scale circulation depends on the season, location, and variable considered. The procedure allows to reconstruct several important ecosystem inputs on a yearly to decadal timescale reasonably well.

The most reliably reconstructed variables were seasonal daily mean, mean minimum and mean maximum temperatures, whereas the poorest results were obtained for daily mean temperature amplitudes, relative humidities, wind speeds, and, for summer only, daily precipitation totals, numbers of days with precipitation above 1mm, plus most within-season standard deviations of daily variables. Some observed 80-year trends, especially for mean daily temperatures and temperature extrema in winter, and for mean minimum temperatures in summer, could not be correctly reproduced at all. All in all most variables were better reconstructed in winter than in summer.

On average over all variables, the three north alpine locations (Bern, Davos and Saentis) could be better linked to large-scale climate than the two more southern locations (Bever, Lugano). This difference was more pronounced in winter than in summer.

(3) The downscaling procedure originally proposed by VON STORCH *et al.* (1993) could be improved by including large-scale near-surface temperature anomalies as an additional large-scale predictor. Improvement was possible for almost all variables and generally for all locations considered in this study. The largest improvements were found for seasonal mean temperatures and mean daily temperature extrema, and for the summer season.

(4) The here presented method allows to flexibly derive regionally differentiated, time-dependent climatic change estimates for input variables required by ecosystem models at a much smaller spatial scale than given by the resolution of present GCMs.

However, the following restrictions of this approach must not be overlooked:

– Considerable amounts of data must be available and have to be managed. Required are sufficiently long records of the local variables close enough to the location of interest, simultaneous observations of the large-scale state of the atmosphere in the sector containing this location, as well as corresponding data sets from experiments with GCMs.

– The method assumes that the established statistical relationships remain valid also under future climatic conditions. For example, towards the end of the "IPCC Scenario A"-experiment the GCM-simulated fields undergo changes, which exceed the range of the observations used to fit the statistical models; thus, towards the end of the next century the projected changes in the local variables represent (linear) extrapolations which might not necessarily hold in the real world.

– The downscaled local climatic changes will not be more trustworthy than the underlying GCM-experiments. For example, the relatively modest temperature increases obtained in our study at all locations are a consequence of the relatively small sensitivity of the ECHAM1/LSG-GCM to increased greenhouse-gas concentrations. Local climatic changes should therefore be explored for experiments with other GCMs, an investigation which is easy to accomplish with our method.

In spite of these difficulties, the proposed method represents to our knowledge the best approach currently available to consistently link GCM-simulated climatic changes to ecosystem models. In combination with stochastic weather generators it can be used to derive multivariate climatic change scenarios on a wide range of temporal scales, and yet it allows to attain the high spatial detail particularly required within a mountainous region. Moreover, our approach can be easily adapted to the specific needs emerging from ongoing ecosystem research. Yet, further improvements can be envisaged by downscaling only a reduced set of inputs, by using additional large-scale predictors, and, as recent work showed (GYALISTRAS & FISCHLIN, 1994), by spatial inter- and extrapolation to points with scanty or even no measurements.

5. REFERENCES

ANDERSON, C.W. (1984). *An introduction to multivariate statistical analysis.* 2nd ed., Wiley & Sons, 675p.

BANTLE, H. (1989). *Programmdokumentation Klima-Datenbank am RZ-ETH Zürich*, Schweiz. Meteorol. Anstalt, Zürich.

BARNETT, T., PREISENDORFER, R. (1987). *Origins and levels of monthly and seasonal forecast skills for United States surface air temperatures determined by canonical correlation analysis.* Mon. Wea. Rev. **15**: 1825-1850.

BRIFFA, K.R., JONES, P.D. (1993). *Global surface air temperature variations during the twentieth century: Part 2, implications for large-scale, high-frequency paleoclimatic studies.* The Holocene, **3**: 77-88.

BRZEZIECKI, B., KIENAST, F., WILDI, O. (1993). *Simulated map of the potential natural forest vegetation of Switzerland.* J. Veg. Science **4**: 499-508.

BUGMANN, H. & FISCHLIN, A. (1992). *Ecological processes in forest gap models – analysis and improvement.* In: Teller, A., Mathy, P. & Jeffers, J.N.R. (eds.), Responses of forest ecosystems to environmental changes, Elsevier Applied Science, London and New York, p953-954.

BUGMANN, H. & FISCHLIN, A. (1994). *Comparing the behaviour of mountainous forest succession models in a changing climate.* In: Beniston, M. (ed.), Mountain environments in changing climates. Routledge, London.

CUBASCH, U., HASSELMANN, K., HöCK, H., MAIER-REIMER, E., MIKOLAJEWICZ U., SANTER, B.D., SAUSEN, R. (1992). *Time-dependent greenhouse warming computations with a coupled ocean-atmosphere model.* Clim. Dyn. **8**: 55-69.

DICKINSON, R.E. (1986). *How will climate change? The climate system and modelling of future coimate.* In: Bolin, B., Döös, B.R., Jäger, J. & Warrick, R.A. (eds.), The greenhouse effect, climatic change and ecosystems. Wiley, Chichester a.o. (SCOPE Vol. 29), p206-270.

EHRENDORFER, M. (1987). *A regionalization of Austria's precipitation climate using principal component analysis.* J. Climatol., **7**: 71 - 89.

FISCHLIN, A. (1982). *Analyse eines Wald-Insekten-Systems: Der subalpine Lärchen-Arvenwald und der graue Lärchenwickler Zeiraphera diniana Gn. (Lep., Tortricidae).* Diss. ETH Nr. 6977, 294p.

FISCHLIN, A., BUGMANN, H. & GYALISTRAS, D. (in print). *Sensitivity of a forest ecosystem model to climate parametrization schemes.* To appear in Env. Pollution.

GYALISTRAS, D., FISCHLIN, A. (1994). *Derivation of climatic change scenarios for mountainous ecosystems: a GCM-based method and the case study of Valais, Switzerland.* Systems Ecology ETHZ Report Nr. 19, Zurich.

FLOHN, H., FANTECHI, R. (eds.) (1984). *The climate of Europe: past, present and future.* D. Reidel Publishing Company, Dordrecht etc., 355p.

GATES, W.L., MITCHELL, J.F.B., BOER, G.J., CUBASCH, U., MELESHKO, V.P. (1992). *Climate modelling, climate prediction and model validation.* In: Houghton, J.T., Callander, B.A., Varney, S.K. (eds.), Climate change 1992 - the supplementary report to the IPCC scientific assessment. Cambridge Univ. Press, Cambridge a.o., p97-134.

GATES, W.L., ROWNTREE, P.R., ZENG, Q.-C. (1990). *Validation of climate models.* In: Houghton, J.T., Jenkins, G.J. & Ephraums, J.J. (eds.), Climate change - the IPCC scientific assessment, Report prepared for IPCC by Working Group 1. Cambridge Univ. Press, Cambridge a.o., p99-137.

GENSLER, G.A. (1978). *Das Klima von Graubünden: ein Beitrag zur Regionalklimatologie der Schweiz.* Arbeitsberichte der Schweiz. Meteorol. Zentralanstalt, Nr.77, Zürich.

GIORGI, F., MARINUCCI, M.R., VISCONTI, G. (1990). *Application of a limited area model nested in a general circulation model to regional climate simulatrion over Europe.* J. Geophys. Res., **95**: 18413-431.

GIORGI, F., MEARNS, L.O. (1991). *Approaches to the simulation of regional climate change: a review.* Rev. Geophys. **2**: 191-216.

GLAHN, H.R. (1985). *Statistical weather forecasting.* In: Murphy, A.H. & Katz, R.W. (eds.), Probability, statistics and decision making in the atmospheric sciences. Westview Press, Boulder, p289-366.

HASSELMANN, K., SAUSEN R., MAIER-REIMER, E., VOSS, R. (1992). *On the cold start problem in transient simulations with coupled ocean-atmosphere models.* MPI Report No 83, Max-Planck-Institut für Meteorologie, Hamburg.

HOUGHTON, J.T., JENKINS, G.J. & EPHRAUMS, J.J. (eds.) (1990). *Climate change - the IPCC scientific assessment. Report prepared for IPCC by Working Group 1.* Cambridge Univ. Press, Cambridge a.o., 365p.

HULME, M., WIGLEY, T.M.L., JONES, P.D. (1990). *Limitations of regional clmate scenarios for impact analysis.* In: Boer, M.M. & de Groot, R.S. (eds.), Landscape-ecological impact of climatic change, IOS Press, Amsterdam, p111-129.

JESSEL, I. (1991). *Inventory of available observed data sets.* Tech. Report No. 1, Deutsches Klimarechenzentrum GmbH, Hamburg.

JONES, P.D., BRIFFA, K.R. (1992). *Global surface air temperature variations during the twentieth century: Part 1, spatial, temporal and seasonal details.* The Holocene, **2**: 165-179.

KARL, T.R., WANG, W.-C., SCHLESINGER, M.E., KNIGHT, R.W., PORTMAN, D. (1990). *A method relating General Circulation Model simulated climate to the observed local climate. Part I: seasonal statistics.* J. Clim., **3**: 1053-1079.

KIM,J.W., CHANG,J.T., BAKER,N.L., WILKS,D.S., GATES,W.L. (1984). *The statistical problem of climate inversion: determination of the relationship between local and large-scale climate.* Mon. Wea. Rev. **112**: 2069-2077.

KREYSZIG, E. (1977). *Statistische Methoden und Ihre Anwendungen.* Vandenhoeck & Ruprecht, Göttingen, 451p.

KUTZBACH, J.E. (1967). *Empirical eigenvectors of sea-level pressure, surface temperature and precipitation complexes over North America.* J. Appl. Met. **6**: 791-802.

LISCHKE, H., BLAGO, N. (1990).: *A model to simulate the population dynamics of the codling moth (Cydia Pomonella L.(Lepidoptera, Torticidae)): development and male moth flight.* Acta Horticultura 276: 43-52.

LOUGH, J.M., WIGLEY, T.M.L., PALUTIKOF, J.P. (1984). *Climate and climate impact scenarios for Europe in a warmer world.* J. Clim. and Appl. Met., **22**: 1673-1684.

MANABE, S., SPELMAN, M.J., STOUFFER, R.J. (1992). Transient responses of a coupled ocean-atmosphere model to gradual changes of atmospheric CO2. Part II: Seasonal response. J. Clim. **5**: 105-126.

MANABE, S., STOUFFER, R.J., SPELMAN, M.J., BRYAN, K. (1991). Transient responses of a coupled ocean-atmosphere model to gradual changes of atmospheric CO2. Part I: Annual mean response. J. Clim. **4**: 785-818.

MEARNS, L.O., KATZ, R.W., SCHNEIDER, S.S. (1984). *Extreme high-temperature events: changes in their probabilities with changes in mean temperature.* J. Clim. Appl. Meteorol., **23**: 1601-1613.

PARRY, M.L., CARTER, T.R. & KONJIN, N.T. (eds.) (1988). *The impact of climatic variations on agriculture, Vol. 1: assessments in cool, temperate and cold regions.* Kluwer Academic Publisher, 876p.

PITTOCK, A.B., SALINGER, M.J. (1982). *Towards regional scenarios for a CO2-warmed earth.* Climatic Change, **4**: 23-40.

PREISENDORFER, R.W., ZWIERS, F.W., BARNETT, T.P. (1981). *Foundations of principal component selection rules.* SIO Ref. Series 81-4, Scripps Inst. Ocn., La Jolla, Ca..

ROTH, O., DERRON, J., FISCHLIN, A., NEMECEK, T. & ULRICH, M. (in print). *Implementation and parameter adaptation of a potato crop simulation model combined with a soil water subsystem.* In: van den Broek, B. & Marshall, B. (eds.), Proc. of the 1st Internat. Workshop on Potato Modelling, May 29-31, 1990, International Agricultural Centre Wageningen, The Netherlands. Pudoc, Wageningen.

SCHRöDER, W. (1976). *Zur Populationsökologie und zum Management des Rothirsches (Cervus elaphus L.) dargestellt an einem Simulationsmodell und der Reproduktionsleistung des Rothirschbestandes im Harz.* Habilitationsschrift, Ludwig-Maximilians-Univ., München, 198p.

SCHüEPP, M., SCHIRMER, H. (1977). *Climates of Central Europe.* In: Wallén, C.C. (ed.), Climates of Central and Southern Europe. World Survey of Climatology, Elsevier, Amsterdam-Oxford-New York, p3-74.

SCHWEINGRUBER, F.H. (1988). *Climatic information for the past hundred years in width and density of conifer growth rings..* In: Wanner, H., Siegenthaler, U. (eds), Long and short term variability of climate, Lecture notes in earth sciences, 16. Springer, Berlin etc..

SHUGART, H.H. (1984). *A theory of forest dynamics. The ecological implications of forest succession models.* Springer, New York a.o., 278p.

SMA (1901-80). *Annalen der Schweizerischen Meteorologischen Anstalt.* Schweiz. Meteorol. Anstalt, Zürich.

SPITTERS, C.J.T., VAN KEULEN, H., VAN KRAALINGEN, D.W.G. (1989). *A simple and universal crop growth simulator: SUCROS87.* In: Rabbinge, R., Ward, S.A. & Van Laar, H.H. (eds), Simulation and systems management in crop protection, Pudoc, Wageningen, p147-181.

STOCKTON, C.W., BOGGESS, W.R., MEKO, D.M. (1985). *Climate and tree rings.* In: Hecht, A. D. (ed), Paleoclimate analysis and modeling. John Wiley, New York etc..

SUPIT, I. (1986). *Manual for generation of daily weather data.* Simulation Reports CABO-TT No.7, Centre for Agrobiological Research, Wageningen, 46p.

SWARTZMAN, G.L. & KALUZNY, S.P. (1987). *Ecological simulation primer.* Macmillan Publishing Co., New York.

UTTINGER, H. (1970). *Niederschlag.* Klimatologie der Schweiz, E, 5. bis 8. Teil, Schweiz. Meteorol. Zentralanstalt, Zürich, 162p.

VINNIKOV, K.J. (1986). *Cuvstviteln'nost' Klimata.* Leningrad, 220p.

VON STORCH, H., ZORITA, E., CUBASCH, U. (1993). *Downscaling of global climate change estimates to regional scales: an applicaton to Iberian rainfall in Wintertime.* J. Climate, **6**: 1161-1171.

WERNER, P., VON STORCH, H. (1993). *Interannual variability of Central European mean temperature in January/February and its relation to the large-scale circulation.* Clim. Res. **3**: 195-207.

WIGLEY, T.M.L., JONES, P.D., BRIFFA,K.R., SMITH,G. (1990). *Obtaining sub-grid scale information from coarse-resolution general circulation model output.* J. Geophys. Res., **95**: 1943-1953.

WIGLEY, T.M.L., JONES, P.D., KELLY, P.M. (1980). *Scenario for a warm, high CO2-world.* Nature, **283**: 17-21.

WIGLEY, T.M.L., JONES, P.D., KELLY, P.M. (1986). *Empirical climate studies.* In: B. Bolin et al. (eds), The greenhouse effect, cimatic change and ecosystems. John Wiley, New York, p271-322.

WILKS, D.S. (1989). *Statistical specification of local surface weather elements from large-scale information.* Theor. Appl. Climatol., **40**: 119-134.

WILKS, D.S. (1992). *Adapting stochastic weather generation algorithms for climate change studies.* Clim. Change, **22**: 67-84.

ETH*zürich*

BERICHTE DER FACHGRUPPE SYSTEMÖKOLOGIE
SYSTEMS ECOLOGY REPORTS

Nr./No.

1 FISCHLIN, A., BLANKE, T., GYALISTRAS, D., BALTENSWEILER, M., NEMECEK, T., ROTH, O. & ULRICH, M. (1993, 2. korr. und erw. Aufl.): Unterrichtsprogramm "Weltmodell 2". 34pp. doi: 10.3929/ethz-a-004271259

1 FISCHLIN, A., BLANKE, T., GYALISTRAS, D., BALTENSWEILER, M., NEMECEK, T., ROTH, O. & ULRICH, M. (2010, 3. korr. Aufl.): Unterrichtsprogramm "Weltmodell 2". 36pp. doi: 10.3929/ethz-b-000729485

2 FISCHLIN, A. & ULRICH, M. (1990): Unterrichtsprogramm "Stabilität". 20pp. doi: 10.3929/ethz-a-004271266

2 FISCHLIN, A. & ULRICH, M. (2010, 2. korr. Aufl.): Unterrichtsprogramm "Stabilität". 20pp. doi: 10.3929/ethz-b-000729486

3 FISCHLIN, A. & ULRICH, M. (1990): Unterrichtsprogramm "Drosophila". 13pp. doi: 10.3929/ethz-a-004271268

3 FISCHLIN, A. & ULRICH, M. (2010, 2. korr. Aufl.): Unterrichtsprogramm "Drosophila". 16pp. doi: 10.3929/ethz-b-000729487

4 ROTH, O. (1990): Maisreife - das Konzept der physiologischen Zeit. 5pp. doi: 10.3929/ethz-b-000728532

5 FISCHLIN, A., ROTH, O., BLANKE, T., BUGMANN, H., GYALISTRAS, D. & THOMMEN, F. (1990): Fallstudie interdisziplinäre Modellierung eines terrestrischen Ökosystems unter Einfluss des Treibhauseffektes. 35pp. doi: 10.3929/ethz-b-000728533

6 FISCHLIN, A. (1990): On Daisyworlds: The Reconstruction of a Model on the Gaia Hypothesis. 19pp. doi: 10.3929/ethz-b-000728534

7 [1*] GYALISTRAS, D. (1990): Implementing a One-Dimensional Energy Balance Climatic Model on a Microcomputer *(out of print)*

8 FISCHLIN, A., & ROTH, O., GYALISTRAS, D., ULRICH, M. UND NEMECEK, T. (1990): ModelWorks - An Interactive Simulation Environment for Personal Computers and Workstations *(for new edition see Systems Ecology Report 14)*. 174pp. doi: 10.3929/ethz-b-000728535

9 FISCHLIN, A. (1990): Interactive Modeling and Simulation of Environmental Systems on Workstations. 16pp. doi: 10.3929/ethz-b-000728536

10 ROTH, O., DERRON, J., FISCHLIN, A., NEMECEK, T. & ULRICH, M. (1992): Implementation and Parameter Adaptation of a Potato Crop Simulation Model Combined with a Soil Water Subsystem. 30pp. doi: 10.3929/ethz-b-000728537

11[*] NEMECEK, T., FISCHLIN, A., ROTH, O. & DERRON, J. (1993): Quantifying Behaviour Sequences of Winged Aphids on Potato Plants for Virus Epidemic Models. 16pp. doi: 10.3929/ethz-b-000728538

---

[*] Out of print

12   FISCHLIN, A. (1991): Modellierung und Computersimulationen in den Umweltnaturwissenschaften. 13pp. doi: 10.3929/ethz-b-000728539

13   FISCHLIN, A. & BUGMANN, H. (1992): Think Globally, Act Locally! A Small Country Case Study in Reducing Net CO2 Emissions by Carbon Fixation Policies. 9pp. doi: 10.3929/ethz-b-000728540

14   FISCHLIN, A., GYALISTRAS, D., ROTH, O., ULRICH, M., THÖNY, J., NEMECEK, T., BUGMANN, H. & THOMMEN, F. (1994): ModelWorks 2.2 – An Interactive Simulation Environment for Personal Computers and Workstations. 324pp. doi: 10.3929/ethz-b-000728541

15   FISCHLIN, A., BUGMANN, H. & GYALISTRAS, D. (1992): Sensitivity of a Forest Ecosystem Model to Climate Parametrization Schemes. 27pp. doi: 10.3929/ethz-b-000728542

16   FISCHLIN, A. & BUGMANN, H. (1993): Comparing the Behaviour of Mountainous Forest Succession Models in a Changing Climate. 14pp. doi: 10.3929/ethz-b-000728543

17   GYALISTRAS, D., STORCH, H. v., FISCHLIN, A., BENISTON, M. (1994): Linking GCM-Simulated Climatic Changes to Ecosystem Models: Case Studies of Statistical Downscaling in the Alps. 33pp. doi: 10.3929/ethz-b-000728544

18   NEMECEK, T., FISCHLIN, A., DERRON, J. & ROTH, O. (1993): Distance and Direction of Trivial Flights of Aphids in a Potato Field. 13pp. doi: 10.3929/ethz-b-000728545

19   PERRUCHOUD, D. & FISCHLIN, A. (1994): The Response of the Carbon Cycle in Undisturbed Forest Ecosystems to Climate Change: A Review of Plant–Soil Models. 29pp. doi: 10.3929/ethz-b-000728546

20   THÖNY, J. (1994): Practical considerations on portable Modula 2 code. 6pp. doi: 10.3929/ethz-b-000728547

21   THÖNY, J., FISCHLIN, A. & GYALISTRAS, D. (1994): Introducing RASS - The RAMSES Simulation Server. 32pp. doi: 10.3929/ethz-b-000728548

22   GYALISTRAS, D. & FISCHLIN, A. (1996): Derivation of climate change scenarios for mountainous ecosystems: A GCM-based method and the case study of Valais, Switzerland. 23pp. doi: 10.3929/ethz-b-000728549

23   LÖFFLER, T.J. (1996): How To Write Fast Programs. 20pp. doi: 10.3929/ethz-b-000728550

24   LÖFFLER, T.J., FISCHLIN, A., & ULRICH, M. (1996): Benchmark Experiments on Workstations. 40pp. doi: 10.3929/ethz-b-000728551

25   FISCHLIN, A., LISCHKE, H. & BUGMANN, H. (1995): The Fate of Forests In a Changing Climate: Model Validation and Simulation Results From the Alps. 18pp. doi: 10.3929/ethz-b-000728552

26   LISCHKE, H., LÖFFLER, T.J., FISCHLIN, A. (1996): Calculating temperature dependence over long time periods: Derivation of methods. 19pp. doi: 10.3929/ethz-b-000728553

27   LISCHKE, H., LÖFFLER, T.J., FISCHLIN, A. (1996): Calculating temperature dependence over long time periods: A comparison of methods. 14pp. doi: 10.3929/ethz-b-000728554

28   LISCHKE, H., LÖFFLER, T.J., FISCHLIN, A. (1996): Aggregation of Individual Trees and Patches in Forest Succession Models: Capturing Variability with Height Structured Random Dispersions. 16pp. doi: 10.3929/ethz-b-000728555

29   FISCHLIN, A., BUCHTER, B., MATILE, L., AMMON, K., HEPPERLE, E., LEIFELD, J. & FUHRER, J. (2003): Bestandesaufnahme zum Thema Senken in der Schweiz. Verfasst im Auftrag des BUWAL. 86pp. doi: 10.3929/ethz-b-000728556

30   KELLER, D. (2003): Introduction to the Dialog Machine, 2nd ed. Price,B (editor of 2nd ed). 35pp. doi: 10.3929/ethz-b-000728557

31   FISCHLIN, A. (2011, ed.2): IPCC estimates for emissions from land-use change, notably deforestation. 3pp. doi: 10.3929/ethz-b-000728558

32   FISCHLIN, A. (2010): Leben im und mit dem Klimawandel – Lebensgrundlagen in Gefahr?. 17pp. doi: 10.3929/ethz-b-000728559

33   FISCHLIN, A. (2010): Andreas Fischlin nimmt Stellung zu Fragen rund um die Klimaproblematik - unter Mitwirkung von Markus Hofmann, Christian Speicher, Betty Zucker, Martin Läubli und Jürg Fuhrer. 49pp. doi: 10.3929/ethz-b-000728560

34   FISCHLIN, A. & FISCHLIN-KISSLING, M.M. (2011): Limits to Growth and Courseware «World Model 2». Update and translation of "Unterrichtsprogramm «Weltmodell 2»" by Fischlin, A., T. Blanke, D. Gyalistras, M. Baltensweiler & M. Ulrich, 1993 (Systems Ecology Report No. 1). 41pp. doi: 10.3929/ethz-b-000728561

35   FISCHLIN, A. & ULRICH, M. (2025): Courseware «Stability». Revision and translation of "Unterrichtsprogramm «Stabilität»" by Fischlin, A. & M. Ulrich, 2010 (Systems Ecology Report No. 2). 20pp. doi: 10.3929/ethz-b-000728562

Um die empfohlene Zitierung eines oben aufgeführten Berichts zu erhalten, fügen Sie vor der Seitenzahl als Herausgeber "Terrestrial Systems Ecology, Department of Environmental Systems Science, ETH Zurich", die Adresse "Zurich, Switzerland", den Serientitel "Systems Ecology Report", sowie die Nummer des Berichts ein. Bsp.: / To obtain the recommended citation of a report listed above insert before the number of pages as the publisher "Terrestrial Systems Ecology, Department of Environmental Systems Science, ETH Zurich", the address "Zurich, Switzerland", the series title "Systems Ecology Report" and the number of the report. Ex.:

PERRUCHOUD, D. & FISCHLIN, A. (1994): The Response of the carbon cycle in undisturbed forest ecosystems to climate change: A review of plant–soil models. Terrestrial Systems Ecology, Department of Environmental Systems Science, ETH Zurich, Zurich, Switzerland, Systems Ecology Report No. **19**: 29pp. doi: 10.3929/ethz-b-000728546

Diese Berichte können in gedruckter Form auch bei folgender Adresse zum Selbstkostenpreis bezogen werden / Order any of the listed reports against printing costs and minimal handling charge from the following address:

ETH ZURICH, TERRESTRIAL SYSTEMS ECOLOGY
UNIVERSITÄTSTR. 16, 8092 ZURICH, SWITZERLAND